uOttawa

L'Université canadienne
Canada's university

FACULTÉ DES ÉTUDES SUPÉRIEURES ET POSTOCTORALES

uOttawa

L'Université canadienne
Canada's university

FACULTY OF GRADUATE AND POSDOCTORAL STUDIES

Scott Foreman
AUTEUR DE LA THÈSE / AUTHOR OF THESIS

M.Sc. (Human Kinetics)
GRADE / DEGREE

School of Human Kinetics
FACULTÉ, ÉCOLE, DÉPARTEMENT / FACULTY, SCHOOL, DEPARTMENT

The Dynamic Impact Response of a Hybrid III Head- and Neckform under Four Neck Orientations and Three Impact Locations

TITRE DE LA THÈSE / TITLE OF THESIS

B. Hoshizaki
DIRECTEUR (DIRECTRICE) DE LA THÈSE / THESIS SUPERVISOR

CO-DIRECTEUR (CO-DIRECTRICE) DE LA THÈSE / THESIS CO-SUPERVISOR

Martin Bilodeau

J. Li

Gary W. Slater
Le Doyen de la Faculté des études supérieures et postdoctorales / Dean of the Faculty of Graduate and Postdoctoral Studies

The Dynamic Impact Response of a Hybrid III Head- and Neckform under Four Neck Orientations and Three Impact Locations

Scott G. Foreman

A thesis submitted to:
The Faculty of Graduate and Postdoctoral Studies of the University of Ottawa
In partial fulfillment of the requirements for the degree for the
Master of Science in Human Kinetics.

Advisor
T. Blaine Hoshizaki, PhD

Committee members
Jing Xian Li, PhD
Martin Bilodeau, PhD

December 10, 2010

Faculty of Health Sciences
School of Human Kinetics

University of Ottawa
© Scott G. Foreman, Ottawa, Canada, 2010

Library and Archives Canada

Published Heritage Branch

395 Wellington Street
Ottawa ON K1A 0N4
Canada

Bibliothèque et Archives Canada

Direction du Patrimoine de l'édition

395, rue Wellington
Ottawa ON K1A 0N4
Canada

Your file Votre référence
ISBN: 978-0-494-74136-8
Our file Notre référence
ISBN: 978-0-494-74136-8

NOTICE:

The author has granted a non-exclusive license allowing Library and Archives Canada to reproduce, publish, archive, preserve, conserve, communicate to the public by telecommunication or on the Internet, loan, distribute and sell theses worldwide, for commercial or non-commercial purposes, in microform, paper, electronic and/or any other formats.

The author retains copyright ownership and moral rights in this thesis. Neither the thesis nor substantial extracts from it may be printed or otherwise reproduced without the author's permission.

AVIS:

L'auteur a accordé une licence non exclusive permettant à la Bibliothèque et Archives Canada de reproduire, publier, archiver, sauvegarder, conserver, transmettre au public par télécommunication ou par l'Internet, prêter, distribuer et vendre des thèses partout dans le monde, à des fins commerciales ou autres, sur support microforme, papier, électronique et/ou autres formats.

L'auteur conserve la propriété du droit d'auteur et des droits moraux qui protège cette thèse. Ni la thèse ni des extraits substantiels de celle-ci ne doivent être imprimés ou autrement reproduits sans son autorisation.

In compliance with the Canadian Privacy Act some supporting forms may have been removed from this thesis.

While these forms may be included in the document page count, their removal does not represent any loss of content from the thesis.

Conformément à la loi canadienne sur la protection de la vie privée, quelques formulaires secondaires ont été enlevés de cette thèse.

Bien que ces formulaires aient inclus dans la pagination, il n'y aura aucun contenu manquant.

Canada

Abstract

Head injuries are sensitive to impact direction and are relative to the magnitude of linear (g) and rotational (rad/s^2) accelerations (Holbourn, 1943; Kleiven, 2003). This study documented the influence of the Hybrid III headform's geometry and neckform's physical characteristics on the dynamic impact response of the Hybrid III headform at different impact locations.

A Hybrid III head- and neckform was impacted by a linear impactor at 4.2m/s to the front, side and rear locations through the center of gravity. To isolate physical characteristic of the neck on the headform's dynamic impact response, the neck's orientation was positioned about the z (vertical) axis.

Impact location was found to be significantly different across all neck orientations for peak resultant linear ($F(2,107)=65.295$, $p<0.001$) and rotational ($F(2,107)=202.822$, $p<0.001$) acceleration. Neck orientation was found to not be significant for peak resultant linear ($F(3,107)=0.560$, $p=0.642$) and rotational ($F(3,107)=0.169$, $p=0.917$) accelerations.

Understanding the interaction of impact location and neckform characteristics is important for interpreting direct head impact reconstructions using the Hybrid III head- and neckform.

Acknowledgements

I would like to extend my gratitude to my supervisor Dr. Hoshizaki for the continued support over the last couple years. I have learned a great deal under your guidance from the numerous experiences we have shared. You truly are an inspiration.

I would also like to extend my thanks to my colleagues from the Neurotrauma Impact and Science lab: Andrew, Evan, Phil, Marshall, Natalie, Anna, Clara, Al and Quyen. My experience over the last couple years has truly been life changing and I would not have been able to do it without all of you.

Lastly, the support provided by my family, especially my brother Brian, my parents Judy and Steve were instrumental in helping me achieve my academic dreams.

Table of Contents

List of Tables i

List of Figures ii

Chapter 1 Introduction 1

Introduction/ Problem Statement 1

Significance 7

Research Question 8

Objective 8

Research Hypotheses 8

Research Hypotheses: 8

Neckform Orientation H_0 Hypotheses: 9

Impact Location H_0 Hypotheses: 10

Independent Variables 11

Dependent Variables 12

Delimitations 12

Limitations 13

Chapter 2 Literature Review 15

Measures of Injury 16

Linear Acceleration 16

Rotational Acceleration 17

Injury Thresholds 18

Biofidelic Response 19

Testing Standards and Headforms 21

Impact Location 23

Summary 25

Chapter 3 Methodology 26

Apparatus 27

Pneumatic Linear Impactor 27

Hybrid III Headform 27
Hybrid III Neckform 28
Procedure 29
Data Collection 29
Research Design 30
Data Collection 30
Data Filtering 30
Statistical Analyses 30

Chapter 4 Results **32**

Chapter 5 Discussion **41**
Hybrid III Headform Impact Location 41
Geometry 42
Moment of Inertia 43
Hybrid III Neckform Orientation 45
Summary 49

Chapter 6 Conclusion **50**
Research Hypotheses: 51
Neck Orientation H_0 Hypotheses: 52
Impact Location H_0 Hypotheses: 53
Summary 54

References: **55**
Appendix A **58**
Appendix B **61**
Appendix C **68**

List of Tables

Table 1: Research design to test the influence of physical neck characteristics on impact location.....30

Table 2: Peak resultant linear acceleration mean and standard deviation for all impact locations and neck orientations at 4.2m/s.....36

Table 3: Peak resultant rotational acceleration mean and standard deviation for all impact locations and neck orientations at 4.2m/s..... 36

Table 4: Time (seconds) to peak resultant linear acceleration mean and standard deviation for all impact locations and neck orientations at 4.2m/s.....40

Table 5: Time (seconds) to peak resultant rotational acceleration mean and standard deviation for all impact locations and neck orientations at 4.2m/s..... 40

List of Figures

Figure 1: Hybrid III Headform impact locations to test against neckform orientations. 11

Figure 2: Hybrid III head- and neckform on low friction sliding table. 14

Figure 3: NOCSAE twin wire test rig. 21

Figure 4: Monorail drop test. 22

Figure 5: Hybrid III "3-2-2-2" accelerometer array (Padgaonkar, 1975). 26

Figure 6: Linear impactor with pneumatic piston and impacting arm. 27

Figure 7: Hybrid III head- and neckform. 28

Figure 8: Hybrid III neck made from rubber butyl inserts and aluminum discs. 29

Figure 9: Comparison of impact location for each neck condition across peak resultant linear acceleration. 33

Figure 10: Comparison of impact location for each neck condition across peak resultant rotational acceleration. 33

Figure 11: Comparison of neck orientation for each impact location across peak resultant linear acceleration. 34

Figure 12: Comparison of neck orientation for each impact location across peak resultant rotational acceleration. 35

Figure 13: Comparison of impact location for each neck condition across the time to the peak resultant linear acceleration. 37

Figure 14: Comparison of impact location for each neck condition across the time to the peak resultant rotational acceleration. 37

Figure 15: Comparison of neck orientation for each impact location across the time to the peak resultant linear acceleration. 38

Figure 16: Comparison of neck orientation for each impact location across the time to the peak resultant rotational acceleration. 39

Figure 17: Side by side comparison of the Hybrid III head- and neckform with and without the rubber butyl skin showcasing facial landmarks. 42

Figure 18: Dynamic impact response between the Front, Side, and Rear impact locations with each neck orientation condition. Shift to the right represents an increased risk of head injury. 43

Figure 19: Comparison of Linear Acceleration on Impact Location for the Forward 0° Neck Orientation. 44

Figure 20: Comparison of Rotational Acceleration on Impact Location for the Forward 0° Neck Orientation. 44

Figure 21: Quasi-static (100mm/min) comparison of neck orientations of Hybrid III neckform serial number 4859. 46

Figure 22: Comparison of Linear Acceleration on Neck Orientation for the Side 90° impact location.47

Figure 23: Comparison of Rotational Acceleration on Neck Orientation for the Side 90° impact location. 47

Figure 24: Comparison of Linear Acceleration on Neck Orientation for the Rear 180° impact location 48

Figure 25: Comparison of Rotational Acceleration on Neck Orientation for the Rear 180° impact location. 48

Chapter 1

Introduction

Introduction/ Problem Statement

Direct head impacts at various locations result in different types of head injuries based on magnitude and type of dynamic response. Understanding how the human head reacts to direct head impacts and the corresponding dynamic response are important for understanding risk of human head injuries (Kleiven, 2003; Gennarelli et al., 1982). Head impacts produce a three dimensional dynamic response measured as linear and rotational accelerations, which are the result of forces acting on the human skull and brain tissues. Newton's second law (F = ma) states that Force is proportional to mass times acceleration; deductively, as mass remains constant, an increase in acceleration increases the magnitude of force acting on the skull and brain tissues, increasing the risk of brain injury. First classified by Holbourn (1943), linear (g x 9.81m/s^2) and rotational (rad/s^2) accelerations were reported as proportional to the risk of injury. In contact sports, it is impossible to predict where direct head impacts are going to occur on a player. Thus, understanding the dynamic response of direct head impacts at different locations on the head is important for determining the risk of head injury.

In 2001, Zhang, Yang, and King identified differences in skull deformations and relative brain dynamic responses between frontal and lateral impacts. Their research employed finite element analyses to model location specific head impacts depending on skull deformation and material properties of the brain subjected to impact forces (Zhang, Yang & King, 2001; Zhang, Yang, King, 2004). Gennarelli and colleagues had previously performed research on monkeys that led to conclusions that lateral direction rotational accelerations compared to anterior and posterior rotational accelerations are an important contributor to concussion (Gennarelli et al., 1982). This was confirmed by further research performed on monkeys where minor traumatic brain injury (mTBI) was the result of the decreased mechanical impedance of lateral impact locations; described as the ability of skull bone through the coronal plane to resist deformation. The different locations on the skull during direct head impacts yielded different dynamic responses (Gennarelli et al., 1982). Research concerning mechanical impedance and compliance of bone was also conducted by Gurdjian, Hodgson, and Thomas (1970). They concluded that long duration impacts (>0.005 seconds) predominantly did not create any deflection or bending of the skull whereas short duration impacts (<0.005 seconds) created deflections in the skull (Gurdjian, Hodgson & Thomas, 1970). Contrary to previous research, finite element modelling calculated similar dynamic impact magnitudes of local skull for frontal and lateral impacts respectively at identical velocities of 6.33m/s with a rigid impactor (Zhang, Yang & King, 2001). Explanation for this difference was attributed to the geometry of the head where "the oval-shaped head deforms non-uniformly as the impact location is varied" and a structure undergoing deformation experiences greater energy attenuation decreasing peak resultant accelerations (Zhang, Yang & King, 2001). The application of a full metal headform (FMH) to helmet testing with very low mechanical impedance provides the necessary dynamic response for long duration

acceleration and increased reliability (Hodgson, 1975). This mechanical characteristic of variable skull compliances is not seen in current headforms used in helmet testing; however, steel and magnesium headforms with high mechanical impedance continue to be used. In addition, the unique elliptical shape of the head creates a moment of inertia at different locations. The moment of inertia ($I = mk^2$) varies with how the mass is distributed and its distance from the center of gravity. A decrease in moment of inertia would be the result of a concentrated mass closer to the center of gravity of the head (Robertson, 2004). Each geometric impact location of the headform and the axis of rotation with respect to the neck can have an affect on the dynamic response and the ability of the headform to rotate.

Techniques to prevent and reduce the risk of head injury have been described by Rousseau (2008). Athletes aware of an impending collision are capable of protecting themselves through a combination of muscle tensioning and impact deflection techniques. Muscles around the neck attach to the upper body, skull and individual vertebrae, and allow or restrict movement of the head. This increases resistance for anterior and lateral movement except for posterior movement which are least resistant because of relative musculature (Mertz & Patrick, 1971). An increase in neck compliance (decreased stiffness) decreases linear acceleration and increases rotational acceleration; whereas a decrease in neck compliance (increased stiffness) increases linear acceleration and decreases rotational acceleration (Rousseau, 2008). The mechanical characteristic of compliance provided by neck muscles in six degrees of freedom during location specific impacts affects the dynamic response across all anatomical planes. Research concerning the dynamic impact response at different locations on the skull during impact is important for identifying the impact dynamic response of the Hybrid III while controlling the physical characteristics of the neck (Nusholtz et al., 1979; Gennarelli et al., 1982; Hodgson et al., 1983;

Zhang, Yang & King, 2001; Kleiven, 2003). The physical characteristics of the Hybrid III neck provide six degrees of freedom for movement of the Hybrid III headform. Originally designed for automotive frontal collisions, the neck has only been quantified for sagittal movement in two of six degrees of freedom (Appendix B). As a result, the neck remains an unknown variable for its level of contribution towards the dynamic impact response for direct head impacts on a Hybrid III head- and neckform at different locations. Use of the neck for dynamic testing provides improved dynamic impact response and allows data collection of three-dimensional linear and rotational acceleration data.

Head injury thresholds that include the Gadd Severity Index (GSI) and Head Injury Criterion (HIC) except for the Head Impact Power index (HIP) have not included thresholds for varying impact directions on the head as an overall predictor of head injury. The one advantage of HIP over other thresholds is direction sensitivity despite not being location sensitive (Newman, Schewchenko & Welbourne, 2000). The Head Injury Criterion (HIC) and Gadd Severity Index (GSI) are an integration of single axis or resultant acceleration curves over time, which were derived from catastrophic front impacts on cadavers and mongrel dogs then quantified by Wayne State University to represent an injury threshold for the entire head during impact (Gadd, 1966). Front impacts are not a true representation of the dynamic impact response for other impact locations and are also not considered the most injurious to the head whereas lateral impacts were found to present an increased risk of injury when compared to other locations using identical impact criteria (Gennarelli et al., 1982; Zhang, Yang & King, 2001; Kleiven, 2003). Understanding the dynamic impact response at various locations and the variables that contributor to the dynamic impact response are crucial to the development of an adequate head injury threshold for impact reconstructions.

The headform widely used is the Hybrid III headform consisting of a rubber butyl covered steel skull that demonstrates very little biofidelity (Pellman et al, 2003a). Compliance characteristics and geometry are two variables that have been identified to influence the dynamic impact response of the head at different impact locations. Head impact reconstructions performed by researchers use the Hybrid III headform because it provides a three-dimensional multi-impact solution with very high reliability, this results in decreased biofidelity and validity. The nature of the steel used in the Hybrid III headform does not allow deformation nor provide natural characteristics of the human head during an impact (Hodgson, 1975). It is important to characterize the dynamic response of the Hybrid III headform at different impact locations of the entire headform to ensure a proper interpretation of the impact response to the relative risk of head injury (Deng, 1989).

Location specific impacts have been identified with varying risks of brain injury (Gennarelli et al., 1982; Hodgson, 1983; Kleiven, 2003; Zhang, Yang & King, 2001, 2004; Hodgson, 1975; Holbourn, 1943). Impacts are measured by accelerometers that represent the physical changes affecting the skull and brain including changes in pressure and levels of shear that represent the risk of injury (Holbourn, 1943; Padgaonkar, 1975; Hoskizaki & Brien, 2004). Researchers over the past half century have debated whether linear or rotational acceleration are the primary culprit for the proper identification of risk of head injury. Linear accelerations have consistently been correlated to subdural hematomas (SDH) which are contusions on the brain and skull fractures involving direct high energy impacts (Holbourn, 1943; King, Yang, Zhang & Hardy, 2003; Gurdjian, Lissner & Patrick, 1963). Rotational accelerations have been identified as the primary indicator for an increased risk of concussion and are supported by research

conducted where lateral direction rotational acceleration were more likely to cause loss of consciousness (Gennarelli et al., 1982).

The Hybrid III headform provides a reliable system to measure acceleration for all locations and directions of impacts despite decreased validity and biofidelity. The Hybrid III neckform is an unknown variable that can affect component acceleration of the dynamic impact response for head impacts because of variations due to the neckform's physical characteristics.

The primary objective of this thesis is to investigate the influence of the Hybrid III headform's geometry and neckform's physical characteristics on the dynamic impact response of the Hybrid III headform at different impact locations. The interactions of the Hybrid III headform's dynamic impact response and the Hybrid III neckforms's physical characteristics have not been defined. Describing the dynamic impact response during direct head impact reconstructions at different locations is important when complex analysis is necessary and the tool being used is not completely understood and properly defined for a specific use.

Significance

Research has reported that impact location and direction play an important role in resulting head injuries (Gennarelli et al., 1982; Hoshizaki & Brien, 2004; Kleiven, 2003; Zhang, Yang & King, 2001, 2004). The limited biofidelity of the Hybrid III headform is a concern for researchers who perform head impact reconstructions that use accelerometers to measure and calculate the dynamic impact response. The dynamic impact response is interpreted as the interaction between a material (the skull) that is attached to other material bodies (neck, impactor and brain) and their related responses during a direct impact (Nusholtz, Melvin & Alem, 1979; Nusholtz et al., 1984). The influence of skull compliance and geometry has been identified as variables that affect the risk of head injury at different impact locations (Gennarelli et al., 1982; Gurdjian, Hodgson & Thomas, 1970). Human neck muscle orientations and characteristics influence compliance through all six degrees of freedom similar to the Hybrid III neck where compliance affects the dynamic impact response (Rousseau, 2008; APPENDIX B & C). Head geometry and physical neck characteristics of the Hybrid III head- and neckform are variables that can influence the dynamic impact response during direct impact testing.

Therefore, this thesis is significant in describing whether a Hybrid III headform is capable of differentiating the dynamic response between different impact locations while controlling for neckform orientation (Nusholtz et al., 1984). Documenting the dynamic impact response characteristics of the Hybrid III headform at different impact locations by controlling neckform orientation is important for interpreting data collected during head impact reconstructions. This study documented the influence of the Hybrid III neckform orientation on the dynamic impact response characteristics at different impact locations of the Hybrid III headform.

Research Question

Is the dynamic impact response of a Hybrid III headform affected by impact location and neck characteristics?

Objective

The objective of this thesis is to describe the influence of impact location and neck characteristics on the dynamic response of the Hybrid III headform during an impact.

Research Hypotheses

Impacts particular to the lateral position and stiffer neck characteristics increase the risk of head injury compared to other impact locations and softer neck characteristics (Gennarelli et al., 1982; Zhang, Yang & King, 2001; Kleiven, 2003). The dynamic impact response at each location will be analyzed to determine if it is related to head geometry or neck characteristics by controlling neck orientation about the Z (vertical) axis. The research and null (H_0) hypotheses are the following:

Research Hypotheses:

- The Hybrid III **neckform orientation** will not affect the dynamic response of the different **impact locations**.
- The time to peak of the resultant linear acceleration of the **side impact location** will be shorter than the **front** and **rear impact locations** at all **neckform orientations**.
- The time to peak of the resultant rotational acceleration of the **side impact** location will be shorter than the **front** and **rear impact locations** at all **neckform orientations**.

- Peak resultant linear acceleration of the **side impact location** will be greater than the **front** and **rear impact locations** at the **forward neckform orientation**.
- Peak resultant rotational acceleration of the **side impact location** will be greater than the **front** and **rear impact locations** at the **forward neckform orientation**.
- Peak resultant linear acceleration of the **side impact location** will be greater than the **front** and **rear impact locations** at the **right sideways neckform orientation**.
- Peak resultant rotational acceleration of the **side impact location** will be greater than the **front** and **rear impact locations** at the **right sideways neckform orientation**.
- Peak resultant linear acceleration of the **side impact location** will be greater than the **front** and **rear impact locations** at the **left sideways neckform orientation**.
- Peak resultant rotational acceleration of the **side impact location** will be greater than the **front** and **rear impact locations** at the **left sideways neckform orientation**.
- Peak resultant linear acceleration of the **side impact location** will be greater than the **front** and **rear impact locations** at the **rearward neckform orientation**.
- Peak resultant rotational acceleration of the **side impact location** will be greater than the **front** and **rear impact locations** at the **rearward neckform orientation**.

Neckform Orientation H_0 Hypotheses:

- There will be no significant differences in the peak resultant **linear** acceleration of the headform between **neckform orientations** at the **front impact location**.
- There will be no significant differences in the peak resultant **linear** acceleration of the headform between **neckform orientations** at the **side impact location**.
- There will be no significant differences in the peak resultant **linear** acceleration of the headform between **neckform orientations** at the **rear impact location.**

- There will be no significant differences in the peak resultant **rotational** acceleration of the headform between **neckform orientations** at the **front impact location**.
- There will be no significant differences in the peak resultant **rotational** acceleration of the headform between **neckform orientations** at the **side impact location**.
- There will be no significant differences in the peak resultant **rotational** acceleration of the headform between **neckform orientations** at the **rear impact location.**

Impact Location H_0 Hypotheses:

- There will be no significant differences in the peak resultant **linear** acceleration of the headform between **impact location** and the **forward neckform orientation.**
- There will be no significant differences in the peak resultant **linear** acceleration of the headform between **impact location** and the **sideways neckform orientation.**
- There will be no significant differences in the peak resultant **linear** acceleration of the headform between **impact location** and the **rearward neckform orientation.**
- There will be no significant differences in the peak resultant **rotational** acceleration of the headform between **impact location** and the **forward neckform orientation.**
- There will be no significant differences in the peak resultant **rotational** acceleration of the headform between **impact location** and the **sideways neckform orientation.**
- There will be no significant differences in the peak resultant **rotational** acceleration of the headform between **impact location** and the **rearward neckform orientation.**

Independent Variables

Variables for impact direction were selected based on head impact criteria identified by the National Operating Committee for Sports and Athletic Equipment (NOCSAE) as locations through the center of gravity, further they provided an equal distance of oblique angles from the adjacent impact site and engaged the Hybrid III headform and neckform through right angles. Neckform orientations were selected based on design features to match the right angle impact locations specifically for direct comparison.

1 - *Impact Locations (3)* (NOCSAE, 2003): Front (0°), Side (90°) & Rear (180°);

→ Through the center of gravity of the headform.

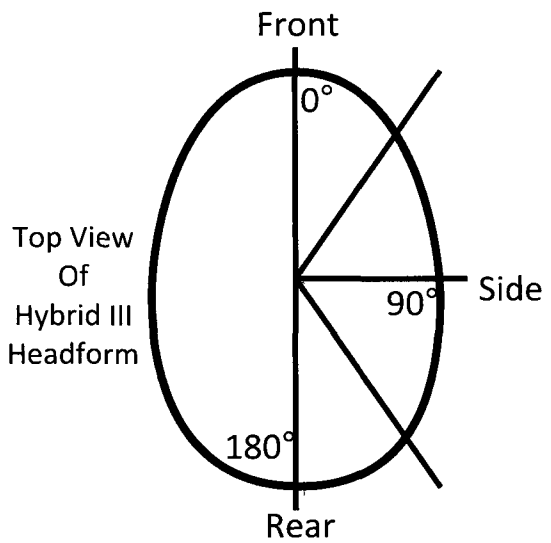

Figure 1: Hybrid III Headform impact locations to test against neckform orientations (NOCSAE, 2006).

2 - *Neck Orientations (4)*: Forward (0°), Right Sideways (+90°), Left Sideways (-90°) & Rearward (180°);

→ About the Z (vertical) axis.

Dependent Variables

The following dependent variables were selected because acceleration is proportional to force which is based on Newton's second law, and is associated with brain tissue damage (Holbourne, 1943). Orthogonally placed accelerometers mounted in a "3-2-2-2" array (Figure 4) in the Hybrid III headform about the center of gravity measured linear accelerations and calculated rotational accelerations during impact (Padgaonkar et al., 1975). The motion and change of velocity of the head is described as the dynamic response defined by:

- Peak resultant linear acceleration (g);
- Peak resultant rotational acceleration (rad/s^2).

Time duration (seconds) to peak of the resultant curve of linear and rotational acceleration is important for describing the moment of inertia of the Hybrid III headform at the three impact locations. Duration of time to the peak of the resultant curves will be described by:

- Time to peak resultant linear acceleration (s);
- Time to peak resultant rotational acceleration (s).

Delimitations

The impact velocity was selected to match methods used in finite modelling and cadaveric testing that showed a progression in skull deflection across a range from 4.36m/s upwards of 12m/s at varying locations (Zhang, Yang & King, 2001; Kleiven, 2003; Nahum, Smith & Ward, 1977). To measure the dynamic response at different locations, the selected velocity of 4.2m/s supported injuries events in sport and were within the normal and safe operating range of the test equipment (Pellman et al., 2003a, 2003b).

Limitations

A 50th percentile Male Hybrid III head and a 50th percentile Hybrid III neckform were used in this thesis as a human surrogate model. Despite its popularity, the Hybrid III headform is not biofidelic and does not imitate the human head's dynamic impact properties although it provides a three-dimensional system for impact measurement (Deng, 1989; Seeman, Muzzy & Lustick, 1986). Furthermore, the Hybrid III neckform was only calibrated for Y axis head rotation and sagittal plane movement (Deng, 1989).

The velocity selected was 4.2m/s to represent an adequate range of possible skull deformation. This range has been identified with levels of concussion in football athletes wearing helmets (Pellman et al., 2003a, 2003b). Due to the high shore value (Shore 60 A) characteristics of the modular elastomer pad (MEP) impacting pad, velocities above this range are beyond the safe operating range of the equipment.

Included with the Hybrid III neck are nodding joints (bump stops) that allow flexion and extension movement of the head about the pin joint before initiation of neck movement (Deng, 1989). These nodding joints are symmetrically placed anteriorly and posteriorly to the pin joint and use a triangular shape to increase stiffness non-linearly through flexion and extension (Deng, 1989). Calibration of the Hybrid III neckform is not performed by the manufacturer to asses lateral bending, and nodding joint structures were only incorporated for anterior and posterior movements (Deng, 1989). A validation of the Hybrid III neckform was performed on an Instron and can be found in Appendix C. As the head is rotated, certain characteristics of the neck are limited by the bump stops for forward and rearward impacts and were considered a single unit.

The Hybrid III headform was outfitted with a rubber butyl skin that provides a more realistic interface between the impactor and the steel skull. The skin is outfitted with features that

accentuate the eye sockets and nose providing approximate landmarks. The orientation of the nose is directly in center for the impactor to hit the center of gravity. The nose may affect the dynamic impact response and as a result may decrease peak resultant linear acceleration and peak resultant rotational acceleration during impact due to its rubber properties acting as an energy attenuator.

The headform is attached to a sliding table (12.78 kg) that allows the Hybrid III headform system to slide backwards after the impact (Figure 2).

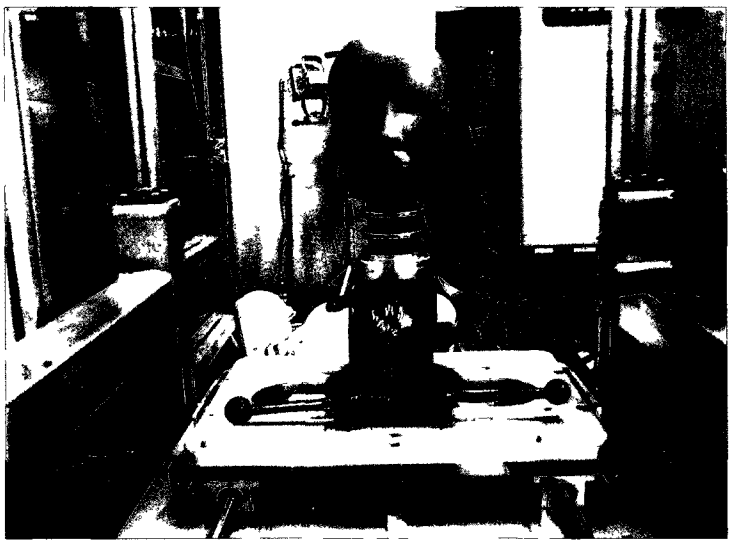

Figure 2: Hybrid III head- and neckform on low friction sliding table.

The table operates on low friction bearings that provide very little resistance to the motion of the dummy, although its effects on the impact dynamics have not yet been studied.

Chapter 2

Literature Review

Helmets were originally made of leather with straps to hold the helmet on the head but provided little or no impact attenuation properties to protect the brain from injury. It was not until 1962 when Sweden introduced the first helmet test standard for ice hockey helmets made from impact absorbing materials (Hoshizaki & Brien, 2004). Canada and the United States were close to follow with not-for-profit organizations like the Canadian Standards Association and American Standards for Testing and Materials that developed standards for helmets that represented the various risks for each sport (Hoshizaki & Brien, 2004). Other standard committees and organizations were conceived in the 1970s including the International Standards Organization (ISO) that eventually developed a testing standard for ice hockey helmets following a 1987 meeting in Ottawa, Ontario, Canada. Discussion from the ISO meeting provided further research helping the National Operating Committee on Standards in Athletic Equipment (NOCSAE) to develop a football helmet test standard (p. 958). Until research is performed in order to develop a biofidelic headform that could provide reliable and valid three-dimensional data rather than the single-dimension biofidelic NOCSAE urethane headform, metal headforms will continue to be the primary tool for measuring impact performances of helmets.

Measures of Injury

Forces and pressures in the brain varying in degree and intensity are produced during direct head impacts (Holbourn, 1943). These forces and pressures are measured as linear and rotational accelerations by headforms outfitted with accelerometers in arrays. Linear and rotational accelerations cannot exist exclusively in nature without the other (Holbourn, 1943; Padgaonkar et al., 1975). Although linear and rotational accelerations reflect changes of force, pressure and shear, acceleration does not directly damage the brain (Holbourn, 1943). Linear accelerations are primarily the main measurement tool in the assessment of helmet performance because it is easy to measure and provides easy comparison of helmet energy attenuating materials (Hoshizaki & Brien, 2004). Using linear acceleration as the primary measurement tool limits the global assessment of injury to the brain and only focuses on the material performance of the helmet. Thus, the application of linear and rotational accelerations should be used in conjunction with each other as parameters in the analysis of traumatic brain injury (TBI) and were used in this thesis to describe the dynamic impact response of a Hybrid III headform.

Linear Acceleration

There has been continued debate concerning the use of linear acceleration to analyze head injuries. The interaction of linear acceleration is believed to be related to the deformation of the skull and resulting pressure gradients during and following head impact (Holbourn, 1943; King, Yang, Zhang & Hardy, 2003). Various studies used monkeys and mongrel dogs to assess levels of linear acceleration and corresponding risk of brain injury. Gurdijan, Lissner, and Patrick (1963) used dogs in their study to analyze traumatic events. They concluded that rotational acceleration did not sufficiently insult the brain to cause injury thus making linear acceleration the superior method for assessment. Ono and colleagues (1980) tested traumatic events on

monkeys and concluded that there is no direct correlation between mTBI and rotational acceleration and that linear acceleration was correlated with mTBIs expressed in monkey brains. Linear accelerations have clinically been associated with focal type contusions and brain hemorrhaging as a result of pressure gradients traveling through the brain during head impacts (Genneralli et al., 1971; 1972).

Rotational Acceleration

Holbourn (1943) was the first to suggest that mTBIs are proportional to the amount of rotational acceleration experienced by the brain. Rotational accelerations are the result of an inertial loading producing both focal and diffuse type injuries on the brain. Shear and tensile strains acting on brain tissue are the mechanisms for diffuse axonal injuries identified by Gennarelli, and Thibault (1982, 1989). Holbourn believed that angular acceleration was primarily responsible for mTBIs and brain hemorrhages (1943). Gennarelli and his colleagues conducted further studies on the role of rotational accelerations on monkey brains (1982). They found that rotational acceleration produced significant diffuse axonal injury from lateral movements and concluded that rotational acceleration alone could cause significant shear stress on brain structures (Gennarelli et al., 1971, 1982; Thibault & Gennarelli, 1989).

The interaction of linear and rotational acceleration during a direct head impact produce focal contusion type injuries and diffuse axonal injuries (Gennarelli et al., 1971, 1982; Thibault & Gennarelli, 1989; King, Yang, Zhang & Hardy, 2003). The contribution of linear acceleration and rotational acceleration to traumatic brain injuries and concussions remains to be identified. The interaction of the brain and skull during direct impact experience a complicated series of events that include relative movement of the brain within the skull, shear strains on brain axons and pressure waves traveling through brain tissue. Since the majority of research describing

linear and rotational accelerations during direct head impacts has been performed on animals, extrapolation to human levels may result in inaccurate thresholds (King, Yang, Zhang & Hardy, 2003.

Injury Thresholds

Linear acceleration thresholds for head injury have been developed by Wayne State University which created a tolerance curve (WSUTC). The Gadd severity index (GSI or SI) is based on the Wayne State Tolerance Curve (WSTC) that is used to predict approximate risk of head injury (Gadd, 1966; Zhang, Yang & King, 2004). The WSTC was developed from high energy impacts at the front location leading to animal and cadaveric skull fractures; when thresholds were identified they were extrapolated to human levels (Gadd, 1966; Zhang, Yang & King, 2004).

Gadd's severity index (GSI) used the original WSUTC and data from another study (Gadd, 1966). The purpose of this new index was to measure the risk of injury within a closed environment similar to the properties of a helmet. It produced a straight curve that had a slope of -2.5 which was used as a weighing factor in the equation (Gadd, 1966).

$$SI = \int_0^t a^{2.5}\, dt$$

This integration is primarily used in the assessment of new helmet technology because of its capability to assess levels of injury within enclosed environments. Values exceeding an SI of 1200, calculated by the GSI were considered unacceptable for new helmets and were also associated with a very high risk of insult to the brain (Gadd, 1966). The primary concern of this criterion is the inability to account for rotational accelerations, deformations of the skull and interacting surfaces of the impact, and the complex movement of the brain within the skull.

Another threshold was developed from data collected from on field impact reconstruction by Pellman et al. during an NFL study (2003). Dynamic impact responses measured by Finite Element Models (FEM) led to thresholds for peak linear "accelerations about the centre of gravity (CG) of the head were estimated to be 66, 82, and 106 G, for a 25%, 50% and 80% probability of mTBI" (Zhang, Yang & King, 2004, p.234). Peak "rotational accelerations for a 25%, 50% and 80% probability of sustaining an mTBI were estimated to be 4.6×10^3, 5.9×10^3, and 7.9×10^3 rad/s^2" (p.234). Further, Hoshizaki and Brien (2004) noted that "accelerations of approximately 80 G have been reported to produce mild traumatic brain injury". Linear accelerations reaching 80 G can be assumed to produce a 50% risk for sustaining an mTBI in the human brain.

Current injury thresholds help to provide researchers with an understanding of the risk of head injury sustained during a head impact. Due to the fact that data supporting these thresholds were gathered from animals and cadavers, based solely on front head impacts and extrapolated to human levels, validity of data from reconstructions are limited by the biofidelity of the equipment being used.

Biofidelic Response

Metal headforms are used at the expense for sacrificing the natural dynamic response of the human head for reliable data (Hoshizaki & Brien, 2004; Hodgson, 1975). The current and most advanced metal headform being used in the head injury industry is the Hybrid III attached to a Hybrid III neck. Outfitted with a "3-2-2-2 array" of accelerometers, the Hybrid III is capable of measuring three-dimensional kinematic data (Padgaonkar et al., 1975). Linear and rotational accelerations are measured during impact providing 3 axes of rotation and 6 degrees of freedom.

The hybrid III head was previously designed for motor vehicle crash reconstructions measuring impulse loading through the neck and was never designed to measure direct impacts (Pellman et al., 2003). As stated by Hodgson (1975) during the development of a new biofidelic head capable of measuring impacts, metal headforms (MHF) were found to be "unrealistic in response characteristics, but also distorted the comparison between helmets thus making a more realistic head model essential." The decreased biofidelity of an impact measurement system is identifiable with the Hybrid III head- and neckform used for direct head impacts because of the steel skull and rubberized skin (Pellman et al., 2003).

Attached to the Hybrid III headform is the Hybrid III neckform. Previously developed for directing impulsive sagittal plane loads to the Hybrid III headform in front end motor vehicle accident reconstructions, the Hybrid III neckform has not been characterized for direct head impacts. Rather, it provides compliance for 6 degrees of freedom for head movement (Deng, 1989). Calibrated against the human neck for flexion and extension movement of the head to provide a realistic response during front impacted motor vehicle accident (MVA), rotation about the transverse plane (Z axis) and coronal plane (Y) are negated during the calibration and design process of the neck (Appendix B) (Deng, 1989). Modelling the Hybrid III neckform to data collected from human trials was difficult because engineers were looking for an impulse response seen in automotive reconstructions rather than applying anatomical data in the development process (Mertz & Patrick, 1971; Deng, 1989). The Hybrid III neckform demonstrated responses that are too stiff compared to human levels; however, headform trajectories during impulsive loading were similar (Seeman, Muzzy & Lustick, 1986). The combination of axes or the coupling of the neck during off-axis directed head impacts further plays a role in the dynamic response of the neck relative to the head. The inclusion of nodding

joints for the anterior-posterior and posterior-anterior movement of the head about the neck pin joint increases the response of the neck and are not factors for lateral and oblique movements of the head about the neck (Deng, 1989).

Testing Standards and Headforms

Different helmets require different standards that are designed to meet the impact demand for each sport. Sports like football, hockey and snow sports require different testing procedures to ensure maximum user safety from head injuries. Football, lacrosse and baseball helmets are tested to a standard outlined by NOCSAE that require a urethane headform outfitted with a helmet that is dropped onto a modular elastomer pad (MEP) at different locations using three uni-axial accelerometers to measure peak linear acceleration and calculate the Gadd Severity Index (NOCSAE, 2005). The half inch MEP pad is designed to represent the type of surface that football players might experience when falling to the ground and hitting their head on the playing surface. Impacts of the headform and helmet to the MEP pad are guided by a twin-wire drop rig that has been designed to limit rotational components and strictly produce linear accelerations from impacts into the ground an infinite mass using gravity (Figure 3).

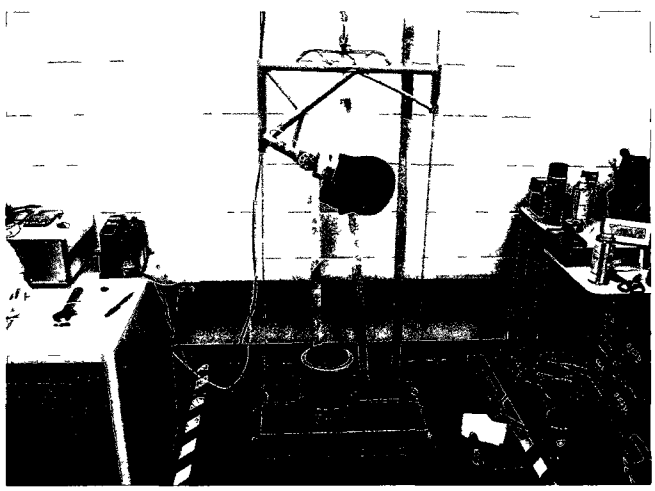

Figure 3: NOCSAE twin wire test rig.

The ASTM has developed a number of test standards used to evaluate helmets used in ice hockey, and non-motorized winter sports like skiing and snowboarding, cycling and football. A monorail style test rig is used to test helmets on a variety of different impact surfaces which limit rotational components while allowing linear acceleration of the headform (Figure 4). These peak linear accelerations are calculated by a single uni-axial accelerometer secured inside a steel or magnesium headform. The helmets are impacted on different surfaces; where hockey helmets are dropped onto a 1 inch thick MEP pad (ASTM, 2006a). Non-motorized winter sport helmets are impacted onto a variety of steel anvils (flat, hemispherical and curb stone) to provide different responses to an environment the helmet might experience (ASTM, 2006b).

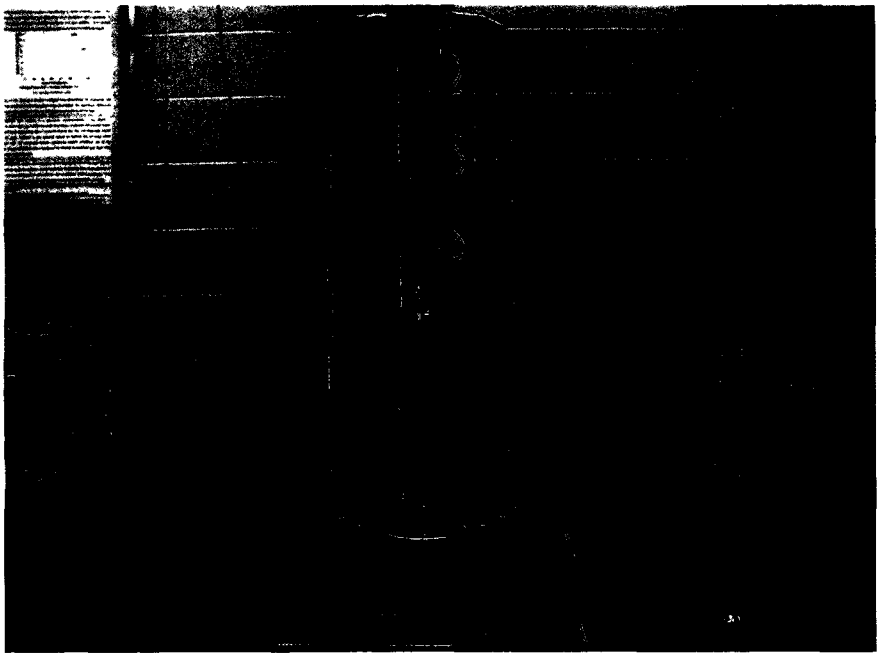

Figure 4: Monorail drop test with magnesium headform.

European and ISO standards use a slightly different test apparatus for alpine and hockey helmets although they still use steel and magnesium head forms. They use a free fall test apparatus with a guided carrier similar to the monorail testing which allows the helmet and headform to respond to the impact on a flat steel anvil inducing a three-dimensional response

(ISO, 2006). A tri-axial accelerometer measures peak linear and rotational accelerations to evaluate impact attenuation properties of the helmet.

NOCSAE has been the first to develop helmet testing standard using the Hybrid III and linear impactor test rig. The proposed standard allows for a fully instrumented and helmeted Hybrid III head- and neckform to be impacted in three-dimensions and provide free motion post impact (NOCSAE, 2006). As defined by NOCSAE to support research that "this test method has been designed to more closely emulate field impacts believed to be responsible for mTBI" (NOCSAE, 2006).

Impact Location

The geometric and material properties of the skull play a role in influencing the impact response on brain tissue. A number of components play a role in the interaction between the striker and the head: hair, scalp, skull, cerebral spinal fluid (CSF) and the brain respectively (Kleiven, 2003). Head impact locations and directions play a role in the types of injuries and their corresponding risk of head injury. Lateral direction and side impacts are more likely to cause diffuse axonal injury which is often the result of rotational accelerations (Gennarelli et al., 1982; Zhang, Yang & King, 2001). Subdural Hematomas (SDH) are brain contusions are a result of linear accelerations and are prevalent in the occipital and frontal region (Zhang, Yang & King, 2001).

Gennarelli and colleagues used monkeys for their study that involved accelerating the head through space by applying a mechanical force instead of a direct impact (1982). Different directions of rotation could be produced on the head that resulted in comas that lasted from several minutes to greater than 6 hours. High correlations were identified between direction of head motion and the length of time for coma; identical correlations were identified with the

outcome as well. For sagittal movement, 85% of the monkeys had good recovery, while 84% of the lateral movement group had a persistent coma (>6hr). Lateral head movements were identified with higher levels of axonal injuries citing higher susceptibility to rotational accelerations in that direction (Gennarelli et al., 1982).

Hodgson and colleagues had also used monkeys for direct head impacts applied by a pneumatic impactor to direct impacts at various locations on the monkey to produce recoverable concussions (1983). Similar to Gennarelli et al.'s study in 1982, lateral impacts had produced the longest duration of unconsciousness. Using high speed film analysis, head rotational accelerations for lateral impacts were 26% higher than impacts to the front. They concluded that the dynamic response may be related to the "oval shape" of the head because there are no apparent intracranial anatomic reasons for the difference in risk of injury (Hodgson et al., 1983).

Finite element modelling was used by Zhang, Yang and King to simulate front and lateral head impacts with an identical impact mechanism at 6.33m/s (2001). Lateral impacts were found once again to experience higher levels of positive pressures and higher levels of shear at the core of the brain. The authors concluded that lateral impacts created higher levels of shear, and if shear was directly related to risk of brain injury, lateral impacts have an decreased tolerance to risk of injury therefore increasing the sensitivity to rotational acceleration (2001).

Summary

Research on risk and cause of head injury has provided the basis for understanding the mechanisms present during head injuries. Linear and rotational accelerations are measured in relation to the pressures and shear forces that cause brain injuries depending on the magnitude of the dynamic impact response (Holbourn, 1943). These injuries vary from contusions to strain related axonal injuries, each affecting the brain differently. Several components that have not been well documented are the different dynamic responses for impact locations and their corresponding injuries. The inherent inability for metal headforms to represent a biofidelic dynamic impact response between impact locations is a limiting factor for understanding the risk of head injury.

Chapter 3

Methodology

The main objective of this study was to document the influence of the Hybrid III neck orientation on the dynamic impact response characteristics at different impact locations of the Hybrid III head- and neckform. Unique treatment of the neck about the vertical (z) axis separated the location specific responses of the Hybrid III headform. The Hybrid III neckform and occipital joint were rotated simultaneously to: 0°, -90°, +90° and 180° and the headform was impacted at each location (front, 0°; side, 90°; and rear 180°) (NOCSAE, 2003). Peak linear acceleration was measured using a "3-2-2-2" array of accelerometers mounted orthogonally in the Hybrid III head and rotational accelerations were calculated to describe the dynamic impact response (Figure 5) (Padgaonkar et al, 1975).

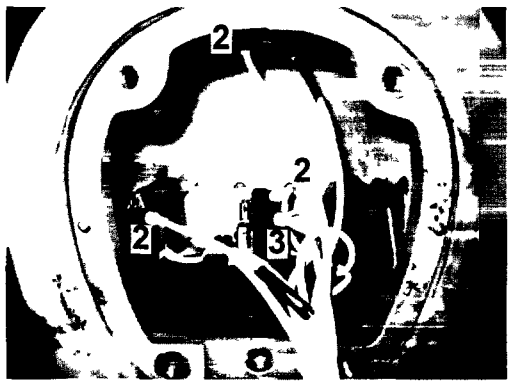

Figure 5: Hybrid III "3-2-2-2" accelerometer array (Padgaonkar, 1975).

Apparatus

Pneumatic Linear Impactor

The pneumatic linear impactor has six major components: pneumatic piston and impacting arm support table, Hybrid III headform mounted to a low friction sliding table, receiving support frame and pneumatic storage tank/adjustable air regulator valve (Figure 6). The horizontally positioned pneumatic piston was fired via an electronically controlled solenoid with air supplied from a storage tank which propels the impacting arm (17.1±0.1 kg) towards Hybrid III head- and neckform mounted to the 6 degree of freedom adjustable sliding table. The sliding table (12.782±0.001 kg), mounted on rails and provides a low friction surface that allowed the system to slide backwards according to the impact. The end of the impacting arm was outfitted with a 1" Shore 60 A MEP impactor.

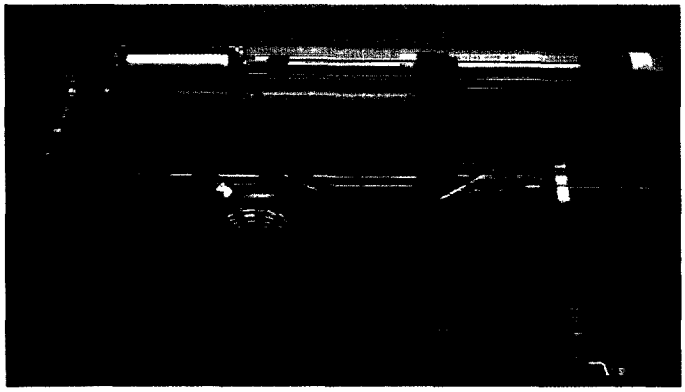

Figure 6: Linear impactor with pneumatic piston and impacting arm.

Hybrid III Headform

A 50th percentile Hybrid III head, with a mass of 4.54±0.01 kg was impacted for this study (Figure 7) (See Appendix A for validation report). Accelerometers were fixed in an orthogonal position near the center of gravity of the headform using the "3-2-2-2" array developed to measure and calculate three-dimensional motion during impact (Padgaonkar, 1975). The center of gravity of the Hybrid III headform is identified as 0.062m about the X axis and

0.036m about the Y axis (Hubbard & Mcleod, 1974). Moment of inertia was also calculated by Willinger et al. to be 0.0159km·m^2 about the X axis and 0.0240km·m^2 about the Y axis (2000). Nine calibrated single axial accelerometers developed by Endevco are mounted in the Hybrid III head and will collect data at 20 KHz.

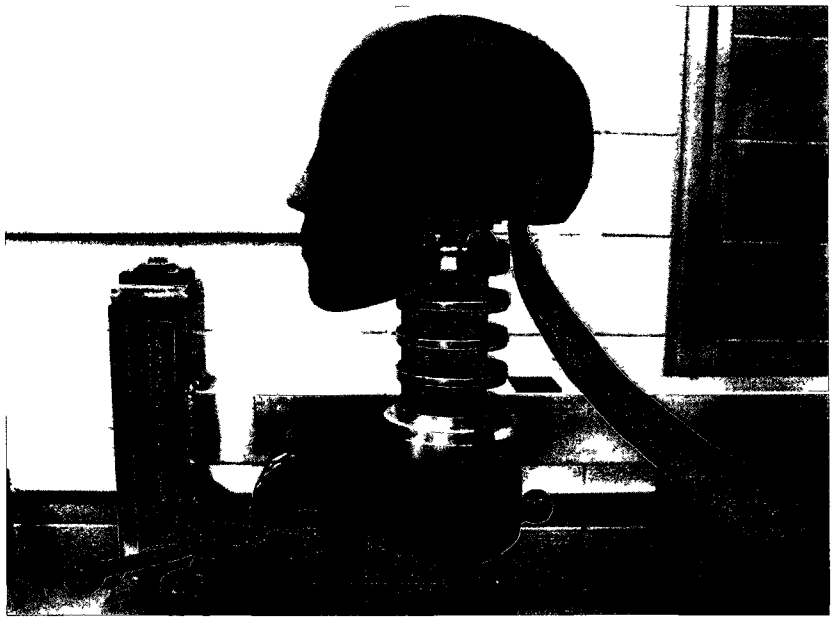

Figure 7: Hybrid III head- and neckform.

Hybrid III Neckform

A 50th percentile Hybrid III neckform with a mass of 1.54±0.01 kg (See Appendix B for validation report), designed with four rubber Butyl discs separated by five aluminum plates, the neck has the ability to simulate human vertebrae and musculature (Figure 8) (Deng, 1989). The rubber discs are offset from the center Z axis by 0.5 cm anteriorly and slit to provide a different response in flexion from extension. No modifications have been engineered for lateral neck movement. The neckform was validated to specification using a neck pendulum and federal regulation number 49 and part 572 for neck flexion and extension movements (APPENDIX B). The Hybrid III neckform was further quantified for flexion, extension and lateral bending to either side, as well as an oblique angle to validate rotation about the Z axis (APPENDIX C).

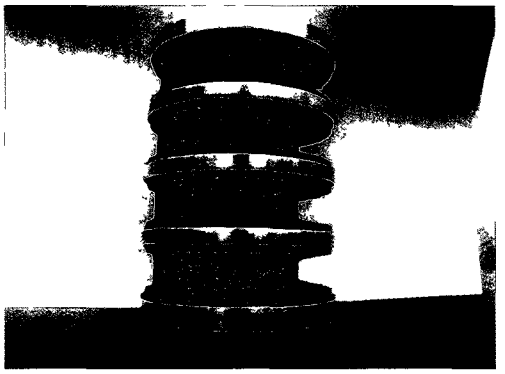

Figure 8: Hybrid III neckform made from rubber butyl inserts and aluminum discs.

Procedure

The effect of physical neckform characteristics on impact location of a 50th percentile Hybrid III headform was analyzed. Prior to each day of testing, the MEP impactor was conditioned on a monorail five times at 5 m/s, consecutively. The Hybrid III head- and neckform was further conditioned by three consecutive impacts using the MEP pad at a velocity of 4.2m/s. The Hybrid III head- and neckform was impacted nine times at each location (front, 0°; side, 90°; and rear, 180°) through the center of gravity at a perpendicular angle to the impact surface for a total of 108 impacts (Figure 1) (NOCSAE, 2003). The Hybrid III neck was fixated in a neutral (vertical) and perpendicular position with reference to the impacting arm for each neck orientation condition (forward, 0°; sideways, -90°; sideways, +90°; and rearward 180°).

Research Design

This thesis was a 3 x 4 fully crossed, balanced research design, to evaluate the influence of impact location and physical neck characteristics on peak resultant linear acceleration, peak resultant rotational acceleration, time to peak resultant linear acceleration and time to peak resultant rotational acceleration. Each condition was tested a total of nine times.

Table 1: Research design to test the influence of physical neck characteristics on impact location.

		Neck Orientation			
		B1	B2	B3	B4
Impact Location	A1	A1B1	A1B2	A1B3	A1B4
	A2	A2B1	A2B2	A2B3	A2B4
	A3	A3B1	A3B2	A3B3	A3B4

A is impact location (3); B is the orientation of the neck (4).

Data Collection

Accelerometer data was collected at 20 KHz by a DTS TDAS module, filtered through a low pass 1000Hz filter specified after SAE J211 Class 1000 filter (SAE, 1995). Instantaneous impact velocity of the impacting arm prior impact was collected by National Instruments VI-Logger and analyzed using Bioproc 2 (data analysis software developed by Dr. D.G.E. Robertson, University of Ottawa, 2008).

Data Filtering

Before any data analysis was performed, all data was filtered using a critically dampened low pass 600Hz digital filter. Several conditions were saturated by noise (mean approximately 400Hz) due to the interaction of the nodding joint and neckform offset at the front location. Bioproc 2 was used to perform the data filtering (data analysis software developed by Dr. D.G.E. Robertson, University of Ottawa, 2008).

Statistical Analyses

Research hypotheses predicting the interaction of neck orientation (forward, 0°; sideways, -90°; sideways, +90°; and rearward 180°) on head impact location (front, 0°; side, 90°; and rear, 180°) a factorial 3x4 analysis of variance (ANOVA) was performed, followed by a post

hoc test (Tukey) when significance was found. The significance level was set at $\alpha = 0.01$. This test was performed to identify the effect of neck orientation on head impact location for peak resultant linear acceleration and peak resultant rotational acceleration. An identical ANOVA was performed to identify the effect of neck orientation on head impact location for time to peak resultant linear acceleration and time to peak rotational acceleration.

All statistical analyses were performed using SPSS 16.0 software (SPSS Inc., Chicago IL, USA).

Chapter 4

Results

Nine impacts were performed at each location (front, 0°; side, 90°; and rear, 180°) for each neck orientation condition (forward, 0°; right sideway, +90°; left sideway, -90°; and rearward 180°). The main effects of impact location on peak resultant linear ($F(2, 107) = 65.295$, $p<0.001$) and peak resultant rotational ($F(2,107) = 202.822$, $p<0.001$) acceleration were significantly different across all conditions for impact location. Results indicated that impact location had a significant effect on peak resultant linear acceleration through the Forward (0°) ($F_{(2, 26)} = 4.47$, $p<0.001$), Left Sideways (-90°) ($F_{(2, 26)} = 310.47$, $p<0.001$), Right Sideways (+90°) ($F_{(2, 26)} = 839.91$, $p<0.001$) and Rearward (180°) ($F_{(2, 26)} = 35.65$, $p<0.001$) neck orientations (Figure 9).

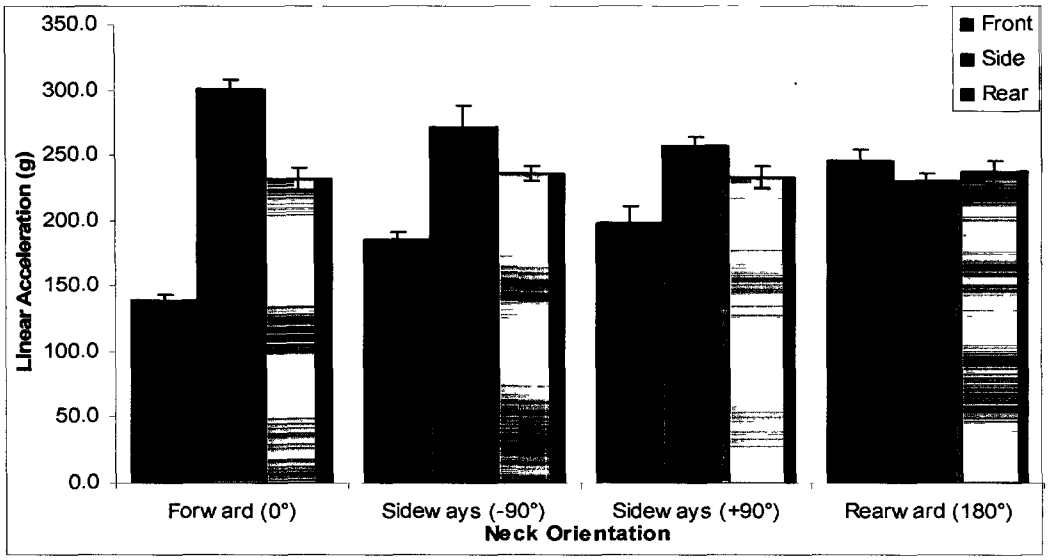

Figure 9: Comparison of impact location for each neck condition across peak resultant linear acceleration.

Peak resultant rotational accelerations were also significant different through the Forward (0°) ($F_{(2, 26)} = 59.30$, $p<0.001$), Left Sideways (-90°) ($F_{(2, 26)} = 2.20$, $p<0.001$), Right Sideways (+90°) ($F_{(2, 26)} = 1.33$, $p<0.001$) and Rearward (180°) ($F_{(2, 26)} = 1.74$, $p<0.001$) neck orientations (Figure 10).

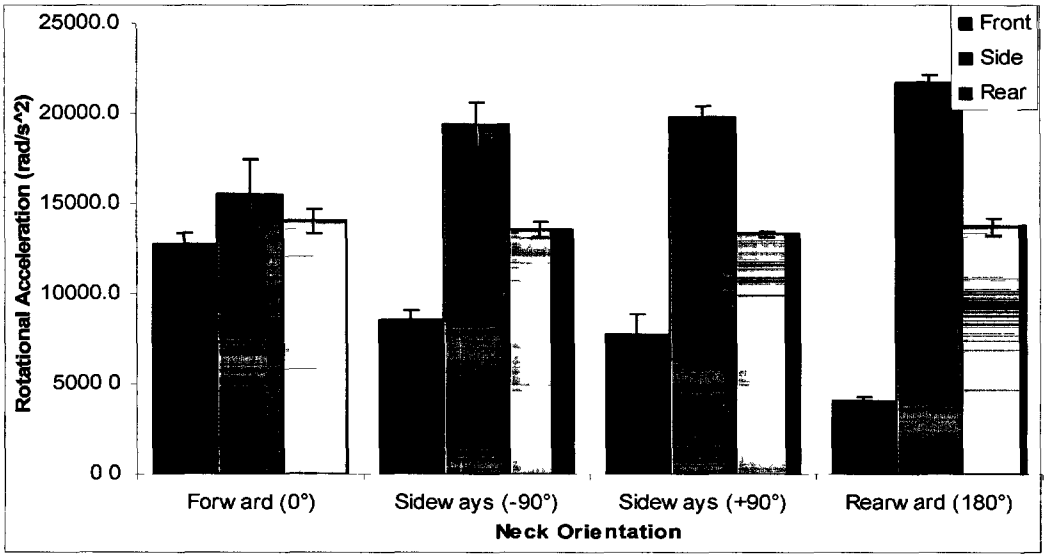

Figure 10: Comparison of impact location for each neck condition across peak resultant rotational acceleration.

Post hoc testing, using Tukey's method, identified significant differences between all locations at all neck orientations ($p<0.01$).

The main effect of neck orientation on peak resultant linear ($F(3,107) = 0.560$, $p=0.642$) and peak resultant rotational ($F(3,107) =0.169$, $p=0.917$) accelerations were found to not be significantly different across neck orientations. Peak resultant linear accelerations at different impact locations were significant at the front ($F_{(2, 35)} = 1.91$, $p<0.001$) and side ($F_{(2, 35)} = 575.99$, $p<0.001$) impact locations. The rear impact location was found to not be significantly different between all neck orientations for peak resultant linear acceleration ($F_{(2, 35)} = 3.34$, $p=0.03$) (Figure 11).

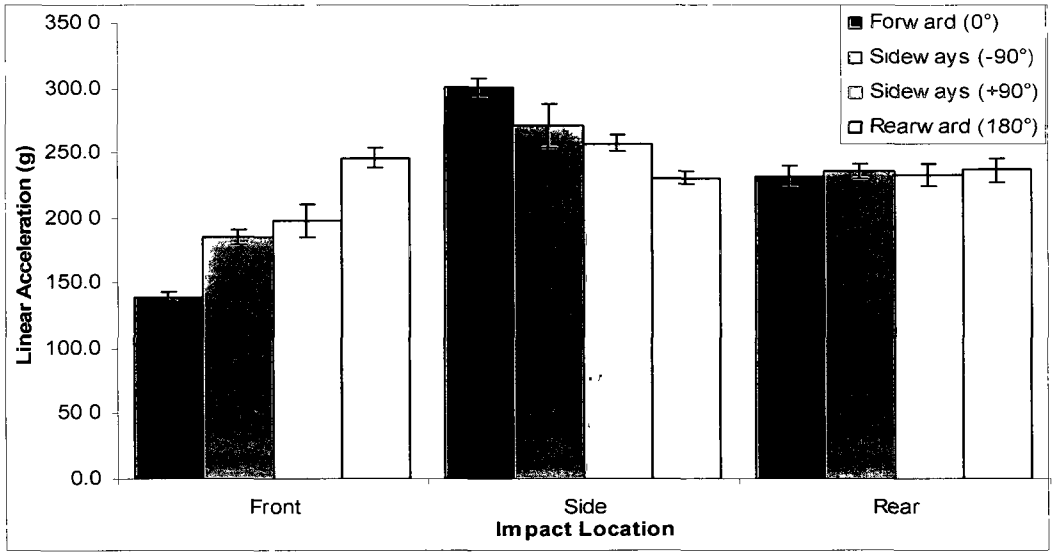

Figure 11: Comparison of neck orientation for each impact location across peak resultant linear acceleration.

Peak resultant rotational acceleration were significantly different at the front ($F_{(2, 35)} = 2.34$, $p<0.001$), side ($F_{(2, 35)} = 184.55$, $p<0.001$) and rear impact location ($F_{(2, 35)} = 17.43$, $p<0.001$) (Figure 12).

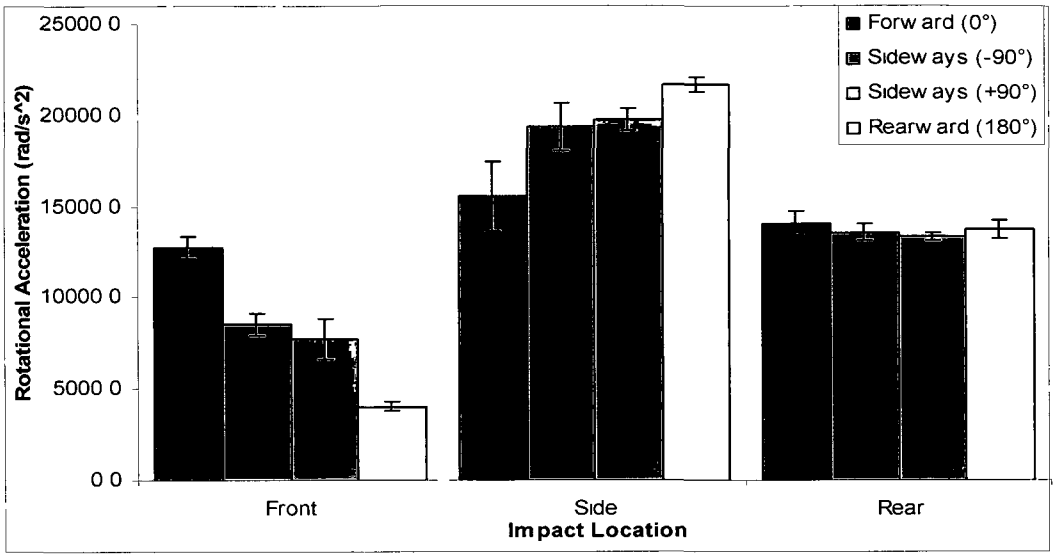

Figure 12: Comparison of neck orientation for each impact location across peak resultant rotational acceleration.

Post Hoc testing using Tukey's method identified no significant difference in peak resultant rotational acceleration between the right and left neck orientation at the side impact location ($p=0.504$). Further Post Hoc testing using Tukey's method identified no significant difference in the peak resultant rotational acceleration between the Right Sideways (+90°) and Left Sideways (-90°) neck orientations at the rear impact locations ($p=0.216$). Further, no significance was found in peak resultant rotational acceleration between the Right Sideways (+90°) and Rearward (180°) neck orientation at the rear impact location ($p=0.568$).

Tables 2 & 3 show the mean and standard deviation for peak resultant linear acceleration and peak resultant rotational accelerations. The results show that fundamentally, the geometry of the Hybrid III headform and Hybrid III neckform characteristics and its physical orientation have an effect on the dynamic impact response of the Hybrid III head- and neckform across all locations except the peak resultant rotational acceleration at the rear impact location.

Table 2: Peak resultant linear acceleration (g) mean and standard deviation for all impact locations and neck orientations at 4.2m/s.

	Impact Location		
Neck Orientation	Front	Side	Rear
Forward (0°)	139.8 ± 1.7	300.6 ± 4.1	232.0 ± 4.2
Right Sideways (+90°)	185.8 ± 2.8	271.0 ± 8.8	236.2 ± 3.0
Left Sideways (-90°)	198.8 ± 6.5	257.7 ± 3.3	232.9 ± 4.2
Rearward (180°)	246.4 ± 4.1	231.2 ± 2.7	237.1 ± 4.6

Table 3: Peak resultant rotational acceleration (rad/s^2) mean and standard deviation for all impact locations and neck orientations at 4.2m/s.

	Impact Location		
Neck Orientation	Front	Side	Rear
Forward (0°)	12759.8 ± 289.2	15532.1 ± 963.7	14071.5 ± 335.7
Right Sideways (+90°)	8525.6 ± 299.5	19362.3 ± 649.2	13576.6 ±225.3
Left Sideways (-90°)	7771.5 ± 564.3	19766.6 ± 307.3	13351.1 ± 84.5
Rearward (180°)	4062.0 ± 131.2	21727.1 ± 204.1	13724.9 ± 249.5

The duration of time in seconds to the peak of resultant linear accelerations and peak resultant rotational acceleration curves are a reflection of the radius of gyration of the Hybrid IIII head- and neckform which is its reluctance to turn about the center of gravity. The main effects of impact location on the duration of time in seconds to the peak resultant linear ($F(2, 107) = 616.127$, $p<0.001$) and peak resultant rotational ($F(2,107) = 403.481$, $p<0.001$) acceleration were significantly different across all conditions for impact location. Results indicated that impact location had a significant effect on the time to peak resultant linear acceleration through the Forward (0°) ($F_{(2, 26)} = 4.21$, $p<0.001$), Left Sideways (-90°) ($F_{(2, 26)} = 6.81$ $p<0.001$), Right Sideways (+90°) ($F_{(2, 26)} = 9.18$, $p<0.001$) and Rearward (180°) ($F_{(2, 26)} = 582.81$, $p<0.001$) neck orientations (Figure 13).

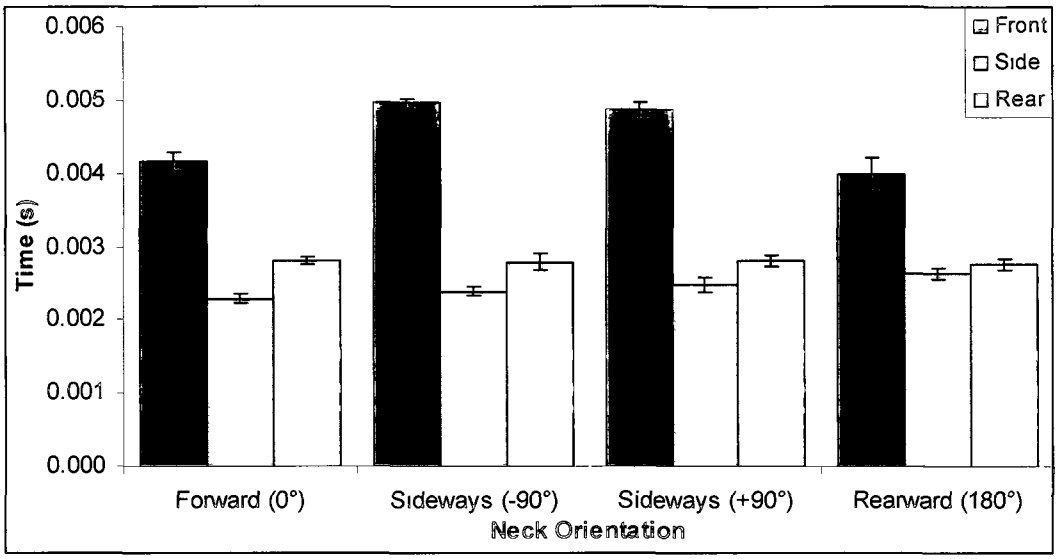

Figure 13: Comparison of impact location for each neck condition across **the time to the peak resultant linear acceleration.**

Time to peak resultant rotational accelerations were also significant different through the Forward (0°) ($F_{(2, 26)} = 2.98$, $p<0.001$), Left Sideways (-90°) ($F_{(2, 26)} = 1.48$, $p<0.001$), Right Sideways (+90°) ($F_{(2, 26)} = 2.36$, $p<0.001$) and Rearward (180°) ($F_{(2, 26)} = 1.23$, $p<0.001$) neck orientations (Figure 14).

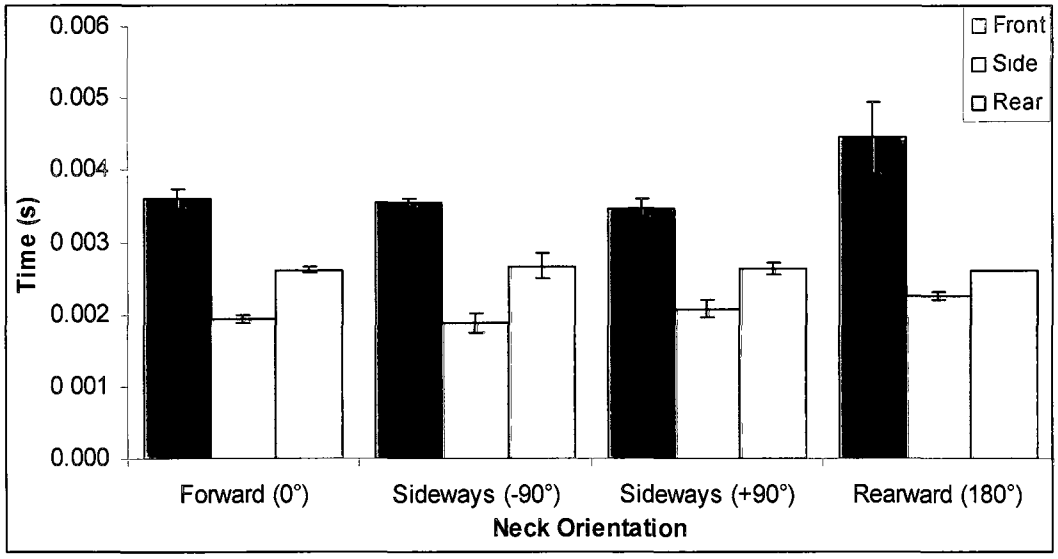

Figure 14: Comparison of impact location for each neck condition across the time to the peak resultant rotational acceleration.

Post hoc testing, using Tukey's method, identified significant differences between all locations at all neck orientations ($p<0.01$).

The main effects of neck orientation the duration of time in seconds to the peak resultant linear ($F(3, 107) = 0.796$, $p<0.001$) and peak resultant rotational ($F(3,107) = 1.777$, $p<0.001$) acceleration were significantly different across all conditions for impact location. The effect of neck orientation on the time to peak resultant linear accelerations at different impact locations was significant at the front ($F_{(2, 35)} = 479.62$, $p<0.001$) and side ($F_{(2, 35)} = 127.67$, $p<0.001$) impact locations (Figure 15).

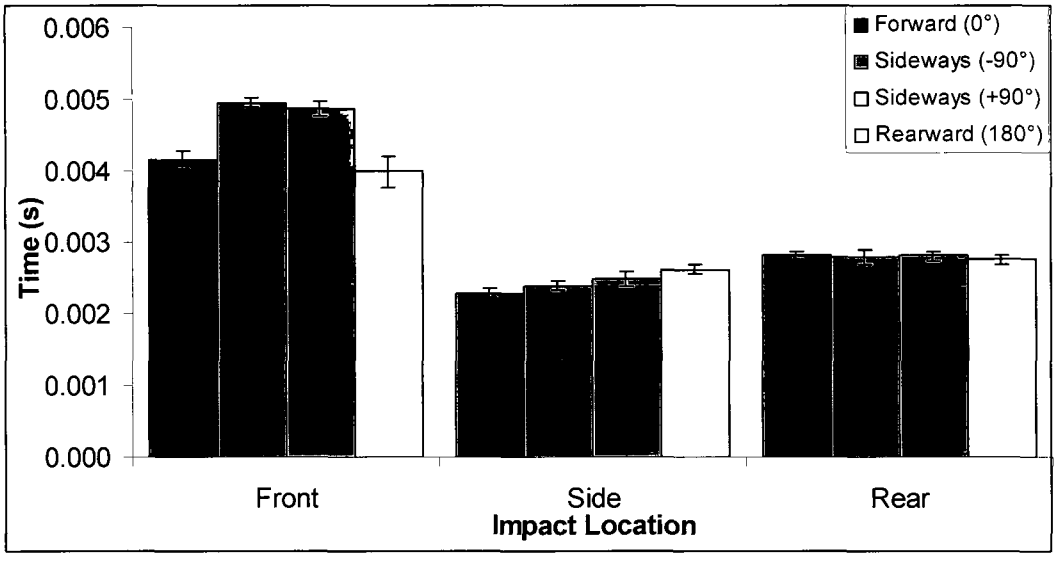

Figure 15: Comparison of neck orientation for each impact location across the time to the peak resultant linear acceleration.

The rear impact location was found to not be significantly different between all neck orientations for the time to peak resultant linear acceleration ($F_{(2, 35)} = 3.60$, $p=0.024$).

The time to peak resultant rotational acceleration was significantly different at the front ($F_{(2, 35)} = 40.60$, $p<0.001$), side ($F_{(2, 35)} = 292.50$, $p<0.001$) impact locations. The rear impact location was found to not be significantly different between all neck orientations for the time to peak resultant rotational acceleration ($F_{(2, 35)} = 3.51$, $p=0.026$) (Figure 16).

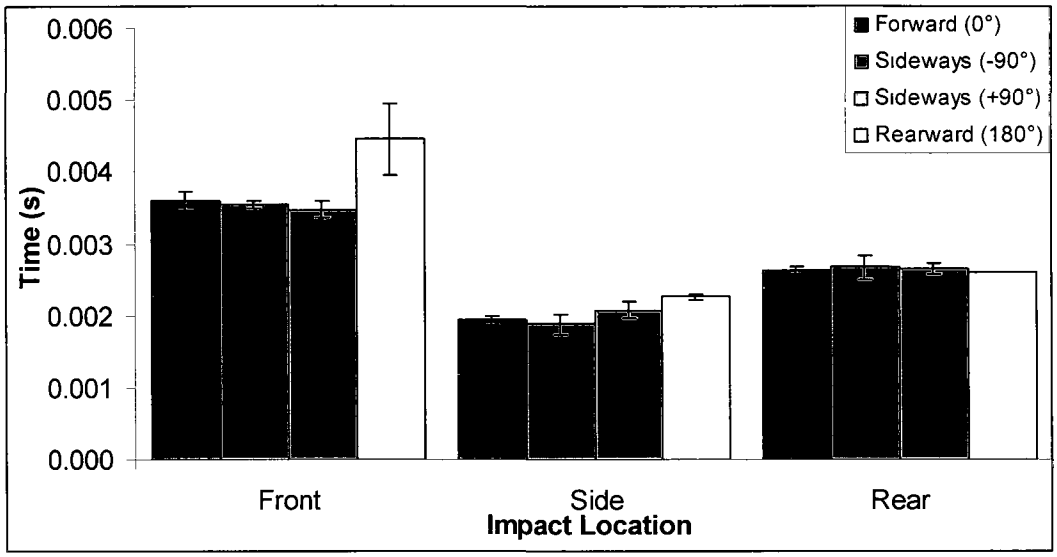

Figure 16: Comparison of neck orientation for each impact location across the time to the peak resultant rotational acceleration.

Post hoc testing, using Tukey's method, identified significant differences between all neck orientations at the Front and Side impact locations for the time to peak resultant linear acceleration ($p<0.05$). Post Hoc testing using Tukey's method identified no significant differences in the time to peak of resultant rotational accelerations between the Forward (180°) and Right Sideways (+90°) ($p=0.861$), Forward (180°) and Left Sideways (-90°) ($p=0.277$) and Left Sideways (-90°) and Right Sideways (+90°) ($p=0.723$) neck orientations at the Front impact locations. No significance was also found in the time to peak of the resultant rotational acceleration between the Forward (180°) and Right Sideways (+90°) neck orientations at the side impact location ($p=0.254$).

The following tables, 4 and 5 show the mean and standard deviation for the time to peak of the resultant linear and resultant rotational acceleration.

Table 4: Time (seconds) to peak resultant linear acceleration (g) mean and standard deviation for all impact locations and neck orientations at 4.2m/s.

	Impact Location		
Neck Orientation	Front	Side	Rear
Forward (0°)	0.00416 ± 0.00007	0.00229 ± 0.00003	0.00282 ± 0.00002
Right Sideways (+90°)	0.00496 ± 0.0003	0.00239 ± 0.00003	0.00279 ± 0.00006
Left Sideways (-90°)	0.00487 ± 0.00006	0.00249 ± 0.00005	0.00281 ± 0.00003
Rearward (180°)	0.00399 ± 0.00011	0.00263 ± 0.00004	0.00276 ± 0.00003

Table 5: Time (seconds) to peak resultant rotational acceleration (rad/s^2) mean and standard deviation for all impact locations and neck orientations at 4.2m/s.

	Impact Location		
Neck Orientation	Front	Side	Rear
Forward (0°)	0.00360 ± 0.00007	0.00193 ± 0.00003	0.00262 ± 0.00003
Right Sideways (+90°)	0.00355 ± 0.00003	0.00188 ± 0.00007	0.00267 ± 0.00009
Left Sideways (-90°)	0.00348 ± 0.00006	0.00208 ± 0.00006	0.00264 ± 0.00004
Rearward (180°)	0.00446 ± 0.00025	0.00226 ± 0.00002	0.00260 ± 0.00000

Chapter 5

Discussion

The purpose of this thesis was to determine if the dynamic impact response of the Hybrid III head- and neckform is the result of headform geometry and neckform physical characteristics. Geometry of the human head is an elliptical shape comprised of bone with variable mechanical impedances and compliances. Geometry plays a role in the moment of inertia where the distance from the center of gravity to the point of impact at different locations about the coronal plane represents the willingness of the headform to rotate about the center of gravity (Robertson, 2008). Neckform physical characteristics are the physical features that include a 5mm offset to the anterior position and various compliances created by the rubber butyl structure (Deng, 1989). This study is the first to characterize the dynamic impact response of a Hybrid III head- and neckform through a fully crossed research design controlling for both Hybrid III headform geometry and Hybrid III neckform characteristics.

Hybrid III Headform Impact Location

The geometry of the Hybrid III headform was designed to specifications of a 50^{th} percentile human male head and produced varying magnitudes of the dynamic response at

different direct impact locations. There are several explanations for separations in the dynamic response between the three impact locations including: moment of inertia of the headform at each location and Hybrid III's geometry and anatomical features.

Geometry

The shape of the Hybrid III headform is an oval shape with the skull and impact surface at varying distances from the center of gravity of the headform. The Hybrid III headform equipped with the rubber butyl skin is also designed with facial landmarks like a nose, lips and eye sockets (Figure 17). These landmarks are crucial to the Hybrid III headform's geometry to

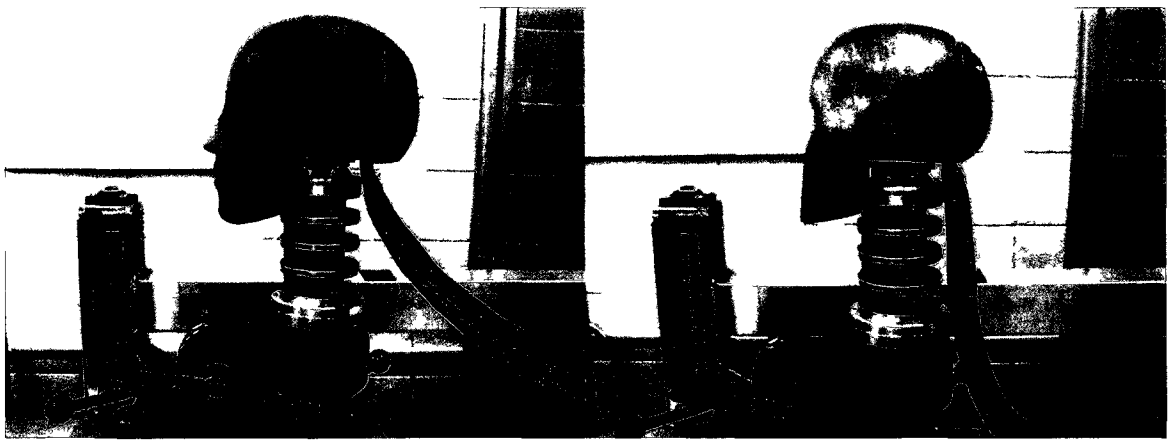

Figure 17: Side by side comparison of the Hybrid III head- and neckform with and without the rubber butyl skin showcasing facial landmarks.

provide a realistic appearance and an appropriate dynamic response of the headform. Hodgson and Nakamura (1968) concluded that facial bones provide energy attenuation properties due to their decreased mechanical impedance unlike the increased mechanical impedance of skull bone. This characteristic of the Hybrid III headform at the front impact location resulted in significantly lower peak resultant linear acceleration and peak resultant rotational accelerations than other impact locations regardless of the neck orientation (Figure 18). Attributed to the decreased magnitude of the dynamic

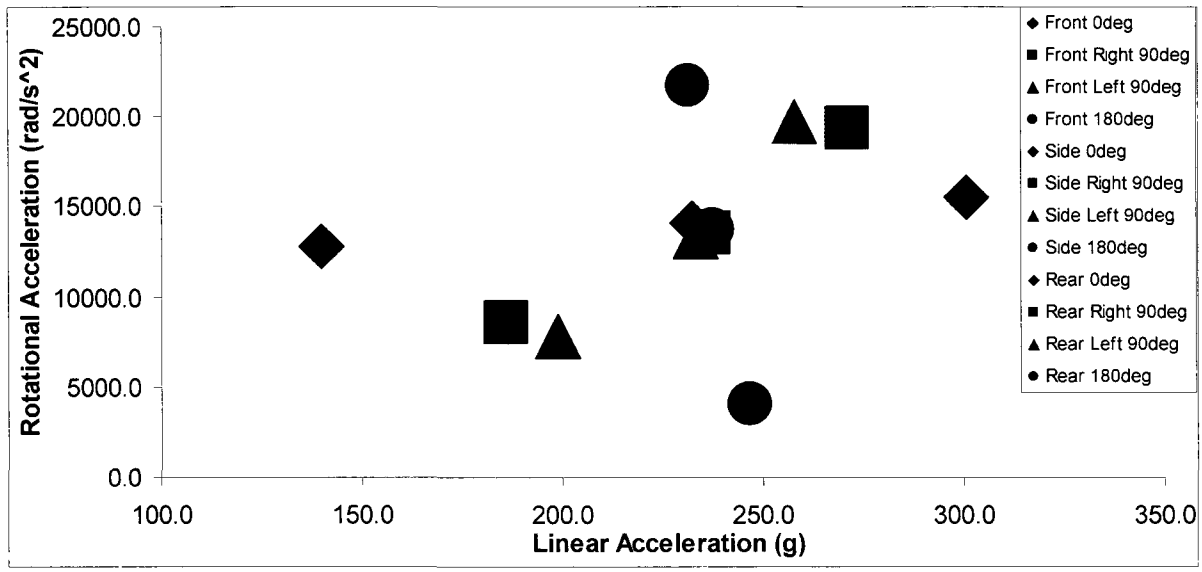

Figure 18: Dynamic impact response between the Front, Side, and Rear impact locations with each neck orientation condition. Shift to the right represents an increased risk of head injury.

response of the Hybrid III headform at the front location was the increased volume and thickness of rubber butyl skin simulating soft tissue often found on the anterior side of the human head that are the Hybrid III headform's landmarks that act to attenuate energy during direct impacts.

Moment of Inertia

The unique oval shape of the Hybrid III headform that distinguishes the different locations may also explain the significant differences in the peak resultant linear acceleration and peak resultant rotational acceleration of the dynamic response between the three impact locations. The front and rear impact locations are approximately (Front location to COG = 0.05588m) the same distance from the center of gravity, and the side impact location (Side location to COG = 0.04826m) is closest to the center of gravity. The k distance (distance to COG), is the factor that affects the magnitude of moment of inertia because the mass of the Hybrid III headform remains constant and never changes (Robertson, 2008). The influence of the Hybrid III headform's geometry is represented in figure 19 & 20, where an identical Forward 0° neck orientation is maintained across all three impact

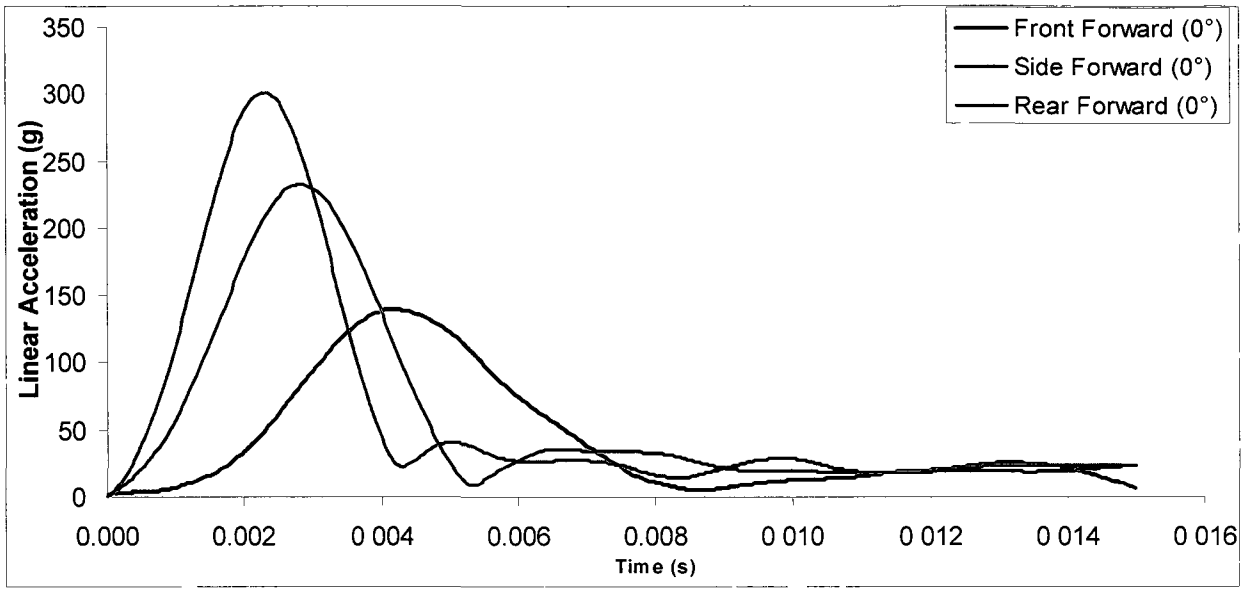

Figure 19: Comparison of Linear Acceleration on Impact Location for the Forward 0° Neck Orientation.

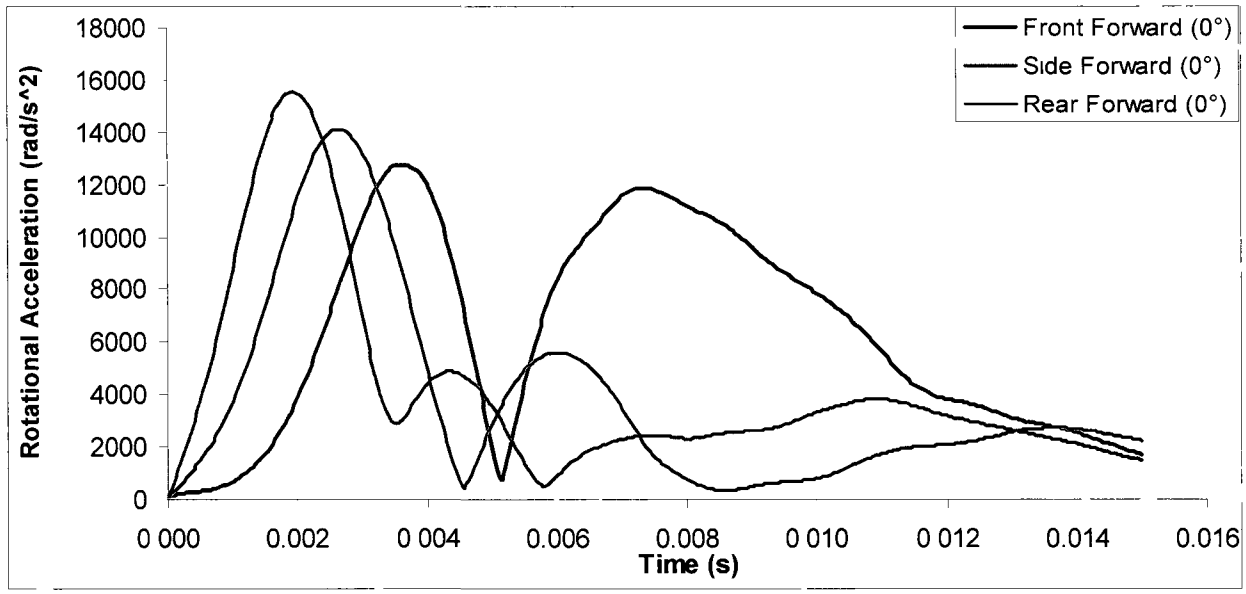

Figure 20: Comparison of Rotational Acceleration on Impact Location for the Forward 0° Neck Orientation.

locations and represent a shift in linear and rotational accelerations. Further, decreases in the time to the peak of the curves for linear and rotational accelerations are evident at the different impact locations where the side k distance is the least, facilitating the rotation about the Y axis. The moment of inertia is the reluctance of an object to turn about the center of gravity

(Robertson, 2008). Time to peak of the resultant linear acceleration and time to peak of the resultant rotational acceleration can describe the shape of the curve and the ability of various locations to rotate and react quicker to a direct impact (Robertson, 2008). Even with an identical neck orientation condition, the shape of the curve between the three impact locations when coupled to the forward 0° neck orientation, shifts to the right and down from the location of the greatest dynamic response magnitude (side impact location).

As previously stated in research, the side impact location was at greater risk of head of head injuries (Gennarelli et al., 1982; Zhang, Yang & King, 2001; Kleiven, 2003). Regardless of neck orientation, the side impact location was at greater risk of injury due to the greater peak linear and rotational accelerations than any other impact location (Figure 17 & 18). A shift to the right in Figure 17 represents a decrease in the k distance, decreasing the moment of inertia, therefore; increasing the risk of head injury. The geometry of the Hybrid III headform has identified directly to research concerning the risk of head injuries at different locations, where side impact locations are at a greater risk of head injury than rear which is also greater than the front impact location (Gennarelli et al., 1982; Zhang, Yang & King, 2001; Kleiven, 2003).

Hybrid III Neckform Orientation

The Hybrid III neckform was originally designed for automotive frontal collisions where an impulse about the sagittal plane was transferred from the body to the Hybrid III headform and the magnitude of the dynamic response was measured (Deng, 1989). Currently, researchers who perform impact reconstructions use the Hybrid III neckform to increase the validity and biofidelity of the impact. As seen in appendix B, dynamic testing of the neck is strictly performed for flexion and extension. Due to the nature of this study, further quasi-static testing

was performed to evaluate the level of compliance across the different orientations (Appendix C). Vasvada et al. found that during resistance, the human neck was strongest during extension, followed by lateral bending and lastly, during flexion (2001). These results are similar to the quasi-static testing that can be found in Appendix C (Figure 21). Previous research that identified an increase in neck stiffness increased linear

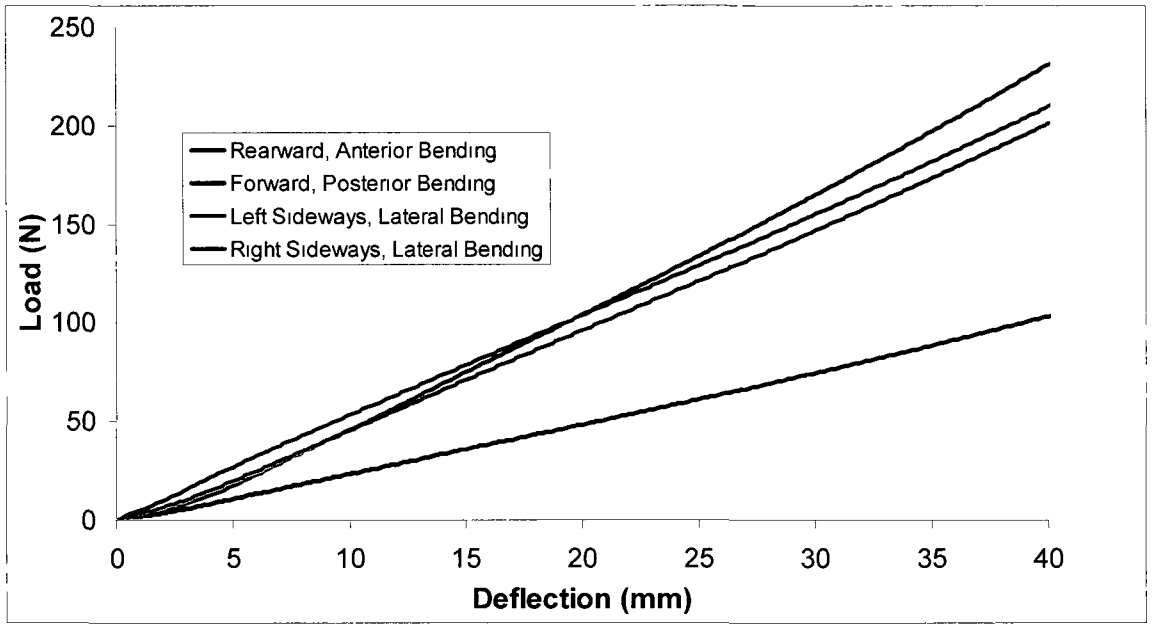

Figure 21: Quasi-static (100mm/min) comparison of neck orientations of Hybrid III neckform serial number 4859.

acceleration and decreased angular acceleration was not apparent when comparing the different neck orientations at different locations. During impacts to the side location, the softest neck orientation (Forward 0°) produced the highest peak linear acceleration (300.1g) as seen in Figure 22 and the lowest peak rotational acceleration (15532.1 rad/s^2) as seen in Figure 23.

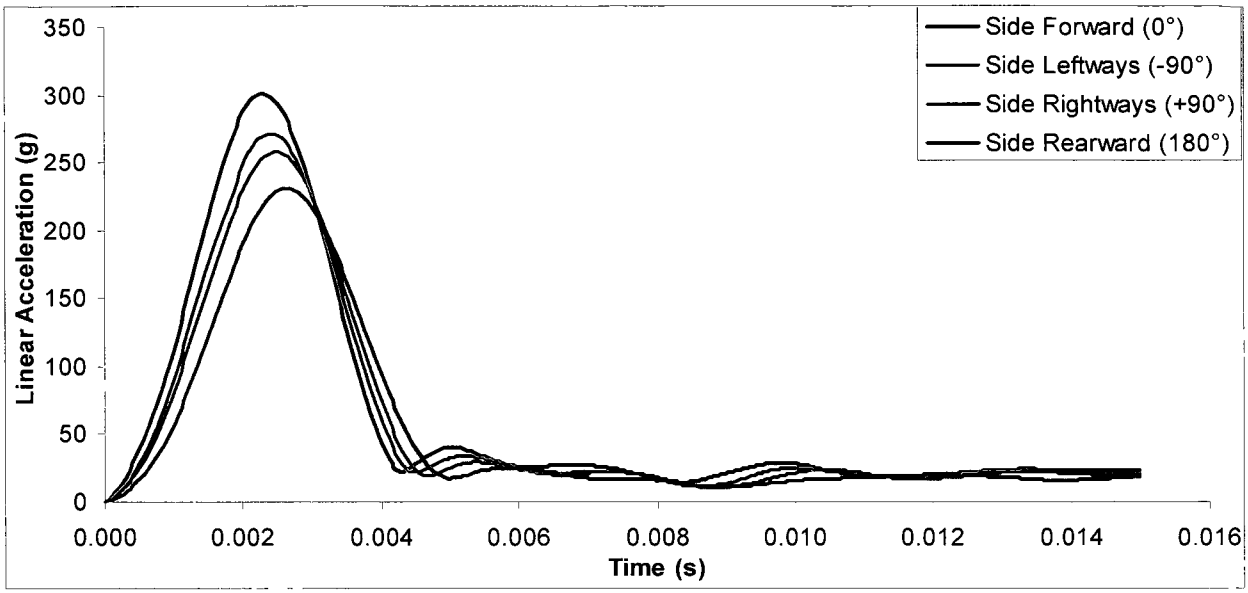

Figure 22: Comparison of Linear Acceleration on Neck Orientation for the Side 90° impact location.

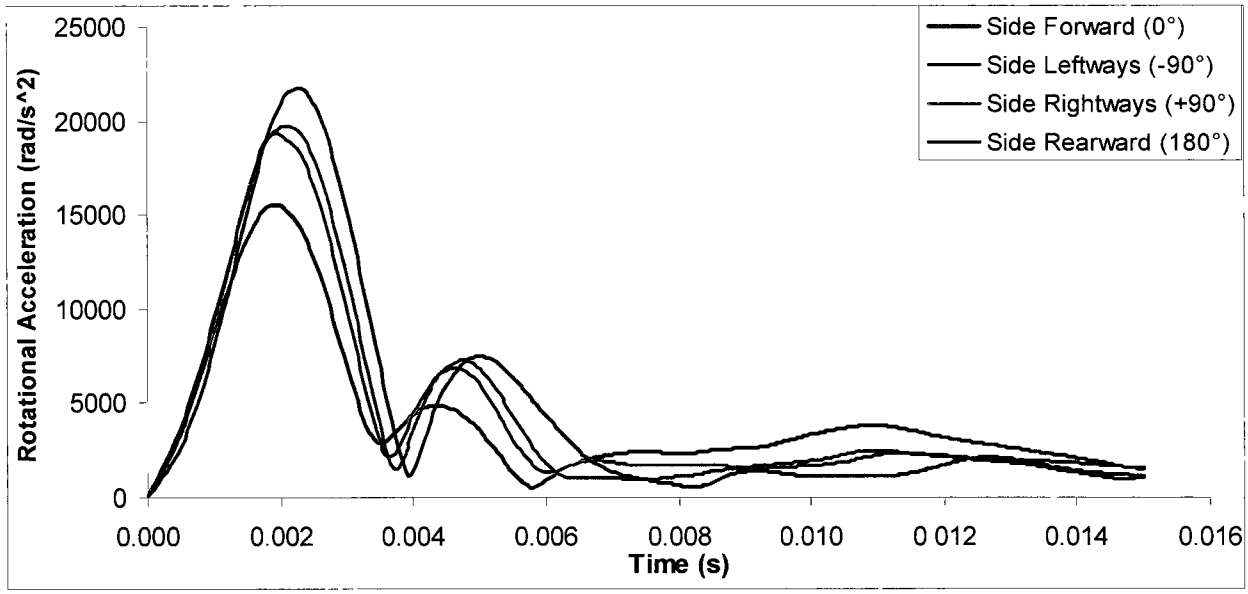

Figure 23: Comparison of Rotational Acceleration on Neck Orientation for the Side 90° impact location.

Similarily, the stiffest neck orientation (Rearward 180°) produced the lowest peak linear acceleration (231.2g) and the highest peak rotational acceleration (21727.1 rad/s^2). However, this trend does not appear at the rear impact location, as peak linear acceleration at the rear impact location was not significantly different between all neckform orientations (Figure 24).

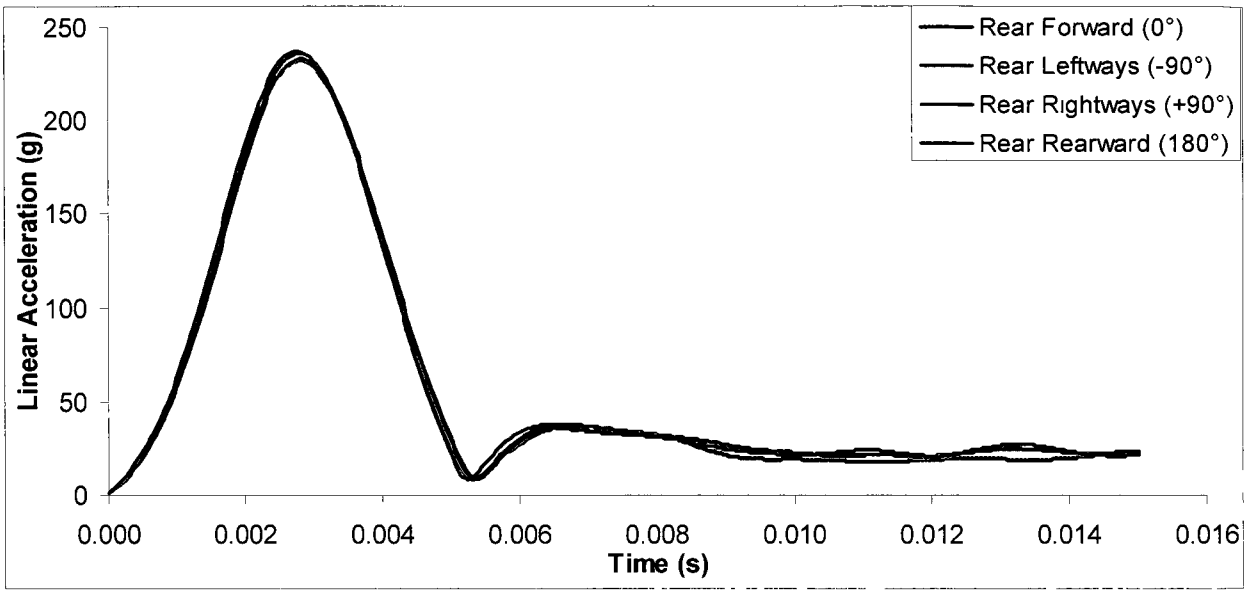

Figure 24: Comparison of Linear Acceleration on Neck Orientation for the Rear 180° impact location.

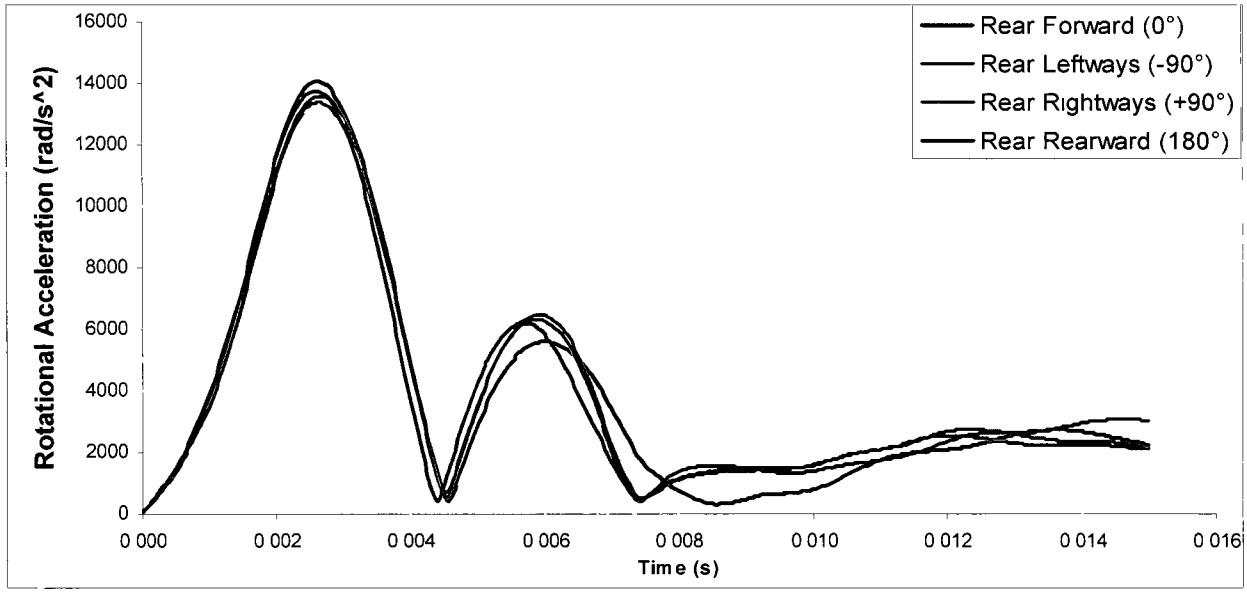

Figure 25: Comparison of Rotational Acceleration on Neck Orientation for the Rear 180° impact location.

Peak rotational acceleration is not significantly different at the rear impact location between the rearward, right sideways and left sideways neck orientations (Figure 25). The possible reason for the rear impact location's inability to distinguish between neck orientations may be that the Hybrid III headform was never designed for direct impacts to the rear impact location and the

back plate that is bolted on may affect the dynamic response beyond the scope of this thesis. The physical characteristics of the Hybrid III neckform allow for an increased level of biofidelity during direct impact at different impact locations and corresponding neck orientations. Further, the theory of neck compliance does not describe the dynamic response adequately between the different neck orientations. A three-dimensional component and sensitivity analysis across all neck orientations is necessary to completely describe the influence of the Hybrid III neckform orientation on the dynamic response of a Hybrid III headform.

Summary

Measuring the amount of time for the resultant linear and rotational acceleration curve to reach the peak value was a critical aspect to understanding the moment of inertia generated by the Hybrid III headform during a direct impact. A decrease in time often resulted in an increase in magnitude of linear and rotational acceleration suggesting an increase in risk of injury at different impact locations, specifically the side impact location. Coupled to the Hybrid III headform, the Hybrid III neckform has also been engineered to simulate the human neck, however; the neckform was never designed for direct impacts and requires quasi-static validation that has proved useful for understanding the type of response of different neck orientations at different head impact locations.

Chapter 6

Conclusion

The objective of this thesis was to determine if the dynamic impact response of the Hybrid III headform was the result of impact location and neck characteristics. It was predicted that impact location and neck orientation would influence the dynamic response of the Hybrid III head- and neckform. The dynamic response of the front impact location was affected by facial features and their low mechanical impedance. The increased dynamic response of the side impact location was influenced by the decreased distance from the impact location to the center of gravity, decreasing the moment of inertia producing a greater risk of injury than other locations of the Hybrid III headform. This finding matches research that identifies the side impact location at greater risk of head injuries (Gennarelli et al., 1982; Zhang, Yang & King, 2001; Kleiven, 2003). The rear impact location was affected by the rear cap of the Hybrid III headform because it was not part of the system and was not designed for direct impact. The physical characteristics of the neckform's different orientations had further influence on the dynamic response of the headform. Understanding these influences is important for developing a three-dimensional head injury protocol and thresholds to continue the advancement of helmet technology with the goal of reducing the risk of head injuries. Understanding the influence of geometry and neck

characteristics on the dynamic response of the Hybrid III head- and neckform is crucial to developing testing protocols and interpreting data from real world impact reconstructions.

Research Hypotheses:

- The Hybrid III neckform orientation will not affect the dynamic response of the different impact locations.

  → Rejected

- The time to peak of the resultant linear acceleration of the side impact location will be shorter than the front and rear impact locations at all neck orientations.

  → Accepted

- The time to peak of the resultant rotational acceleration of the side impact location will be shorter than the front and rear impact locations at all neck orientations.

  → Accepted

- Peak resultant linear acceleration of the side impact location will be greater than the front and rear impact locations at the forward neck orientation.

  → Accepted

- Peak resultant rotational acceleration of the side impact location will be greater than the front and rear impact locations at the forward neck orientation.

  → Accepted

- Peak resultant linear acceleration of the side impact location will be greater than the front and rear impact locations at the right sideways neck orientation.

  → Accepted

- Peak resultant rotational acceleration of the side impact location will be greater than the front and rear impact locations at the right sideways neck orientation.

  → Accepted

- Peak resultant linear acceleration of the side impact location will be greater than the front and rear impact locations at the left sideways neck orientation.

  → Accepted

- Peak resultant rotational acceleration of the side impact location will be greater than the front and rear impact locations at the left sideways neck orientation.

  → Accepted

- Peak resultant linear acceleration of the side impact location will be greater than the front and rear impact locations at the rearward neck orientation.

  → Rejected

- Peak resultant rotational acceleration of the side impact location will be greater than the front and rear impact locations at the rearward neck orientation.

  → Accepted

Neck Orientation H_0 Hypotheses:

- There will be no significant differences in the peak resultant **linear** acceleration of the headform between **neck orientations** at the **front impact location**.

  → Rejected

- There will be no significant differences in the peak resultant **linear** acceleration of the headform between **neck orientations** at the **side impact location**.

  → Rejected

- There will be no significant differences in the peak resultant **linear** acceleration of the headform between **neck orientations** at the **rear impact location.**

  → Accepted

- There will be no significant differences in the peak resultant **rotational** acceleration of the headform between **neck orientations** at the **front impact location**.

  → Rejected

- There will be no significant differences in the peak resultant **rotational** acceleration of the headform between **neck orientations** at the **side impact location**.

  → Rejected

- There will be no significant differences in the peak resultant **rotational** acceleration of the headform between **neck orientations** at the **rear impact location.**

  → Rejected

Impact Location H_0 Hypotheses:

- There will be no significant differences in the peak resultant **linear** acceleration of the headform between **impact location** and the **forward neck orientation.**

  → Rejected

- There will be no significant differences in the peak resultant **linear** acceleration of the headform between **impact location** and the **sideways neck orientation.**

  → Rejected

- There will be no significant differences in the peak resultant **linear** acceleration of the headform between **impact location** and the **rearward neck orientation.**

  → Rejected

- There will be no significant differences in the peak resultant **rotational** acceleration of the headform between **impact location** and the **forward neck orientation.**

  → Rejected

- There will be no significant differences in the peak resultant **rotational** acceleration of the headform between **impact location** and the **sideways neck orientation.**

  → Rejected

- There will be no significant differences in the peak resultant **rotational** acceleration of the headform between **impact location** and the **rearward neck orientation.**

  → Rejected

Summary

This study has provided important information and data concerning the dynamic response of the Hybrid III head- and neckform. Describing headform geometry and physical neckform characteristics of a measurement tool used during impact reconstructions is very important when interpreting data. It is expected that this thesis can be used as a reference for the development of more rigorous three-dimensional head injury thresholds in the development of sports and recreational activity helmets designed to protect the human head from injury.

References

American Society for Testing and Materials, (2006a). Standard performance specification for ice hockey helmets. F1045-06

American Society for Testing and Materials, (2006b). Standard specification for helmets used for recreational snow sports. F2040-06

Deng, Y. (1989). Anthropomorphic dummy neck modeling and injury considerations. *Accident Analysis and Prevention, 21(1),* 85-100

Gadd, C.W. (1966). Use of a weighted impulse criterion for estimating injury hazard. *Proc. 10th Stapp Car Crash Conf.*, 164-174.

Gennarelli, T.A., Ommaya, A.K., & Thibault, L.E. (1971). Comparison of translational and rotational head motions in experimental cerebral concussion. *Proc. 15th Stapp Car Crash Conference*, 797-803.

Gennarelli, T.A., Thibault, L.E. & Ommaya, A.K. (1972). Pathophysiologic response to rotational and linear accelerations of the head. *Proc 16th Stapp Car Crash Conference*, SAE paper number: 720970

Gennarelli, T.A., Thibault, L.E., Adams, J.H., Graham, D.I., Thompson, C.J., & Marcincin, R.P. (1982). Diffuse axonal injury and traumatic coma in the primate. *Annals of Neurology, 12*(6), 564-547.

Gurdjian, E.S., Hodgson, V.R., & Thomas, L.M. (1970). Studies on mechanical impedance of the human skull: Preliminary report. *Journal of Biomechanics, 3*(1), 239-247.

Gurdjian, E.S., Lissner, H.R., & Patrick, L.M. (1963). Concussion-mechanism and pathology. *Proc. 7th Stapp Car Crash Conf.,* 470-482.

Hodgson, V.R. & Nakamura, G.S. (1968). Mechanical impedance and impact response of the human cadaver zygoma. *Journal of Biomechanics, 1*, 73-78.

Hodgson, V.R. (1975). National Operating Committee on Standards for Athletic Equipment football helmet certification program. *Medicine and Science in Sports, 7*(3), 225-232.

Hodgson, V.R. et al. (1983). The role of impact location in reversible cerebral concussion. *Proc. 27th Stapp Car Crash Conf.,* SAE paper number: 831618, 225-240.

Holbourn, A.H.S. (1943). Mechanics of head injury. *Lancet, 2,* 438-441.

Hoshizaki, T.B., & Brien, S.E. (2004). The science and design of head protection in sport. *Neurosurgery, 55,* 956-967.

Hubbard, R.P. & Mcleod, D.G (1972). Definition and development of a crash dummy head. SAE paper number: 741193.

International Organization for Standardization, (2006). Impact drop test using a free-fall apparatus with a guided carrier. FDIS ISO/EN 10256:2005-11-07.

King, A.I., Yang, K.H., Zhang, L., & Hardy, W. (2003). Is head injury cause by linear or rotational acceleration. *IRCOBI Conference*.

Kleiven, S. (2003). Influence of impact direction on the human head in prediction of subdural hematoma. *Journal of Neurotrauma, 20*(4), 365-379.

Mertz, H.J., & Patrick, L.M. (1971). Strength and response of the human neck. *Proc. 15th Stapp Car Crash Conf.,* SAE paper number: 710855.

Nahum, A., Smith, R., & Ward, C. (1977). Intracranial pressure dynamics during head impact. *Proc. 15th Stapp Car Crash Conference*, SAE paper number 770922.

National Operating Committee on Sports and Athletic Equipment, (2003). Laboratory procedural guide for certifying newly manufactured football helmets. NOCSAE DOC (ND) 003-93m03.

National Operating Committee on Sports and Athletic Equipment, (2005). Standard drop test method and equipment used in evaluating the performance characteristics of protective headgear. NOCSAE DOC (ND) 001-04m05.

National Operating Committee on Sports and Athletic Equipment, (2006). Standard linear impactor test method and equipment used in evaluation the performance characteristics of protective headgear and face guards. NOCSAE DOC (ND) 081-04m04.

Newman, J.A., Shewchenko, N., & Welbourne, E. (2000). A proposed new biomechanical head injury assessment function – the maximum power index. *Proc. 44th Stapp Car Crash Conf.,* Stapp paper number: OOS-80.

Nusholtz, G., Melvin, J. & Alem., N. (1979). Head impact response comparisons of human surrogates. *Proc. 21th Stapp Car Crash Conf.,* SAE paper number: 791020.

Nusholtz, G., Lux, P., Kaiker, P., Janicki, M. (1984). Head impact response – Skull deformation and angular accelerations. SAE paper number: 841657.

Ono, K., Kikuchi, A., Nakamura, M., Kobayashi, H., & Nakamura, H. (1980). Human head tolerance to sagittal impact reliable estimation deduced from experimental head injury using sub-human primates to concussion threshold for man. *Stapp Car Crash Journal, 24*, 101-160.

Padgaonkar, A.J., Kreiger, K.W., & King, A.I. (1975). Measurement of angular accelerations of a rigid body using linear accelerometers. *Journal of Applied Mechanics, 42,* 552-556.

Pellman, E.J., Viano, D.C., Tucker, A.M., Casson, I.R., & Waeckerle, J.F. (2003a). Concussion in professional football: Reconstruction of game impacts and injuries. *Neurosurgery, 53,* 799-814.

Pellman, E.J., Viano, D.C., Tucker, A.M., & Casson, I.R. (2003b). Concussion in professional football: Location and direction of helmet impacts – Part 2. *Neurosurgery, 53,* 1328-1341.

Robertson, D. (2004). *Introduction to biomechanics for human analysis: Second edition.* Waterloo, Ontario: Waterloo Basics.

Rousseau, P. (2008). The influence of neck compliance and head displacement on impact dynamics of a Hybrid III head. University of Ottawa (Thesis).

Seeman, M.R., Muzzy, W.H., & Lustick, L.S. (1986). Comparison of human and Hybrid III head and neck dynamic responses. *Stapp Car Crash Journal, 30,* 291-310.

Society of Automotive Engineers, (1995). *Instrumentation for impact test part 1: Electronic instrumentation – SAE J211-1.* Warrendale: Society of Automotive engineers.

Thibault, I.E., & Gennarelli, T.A. (1989). Biomechanics of diffuse brain injuries. *Proc. 10th Int Tech Conf on Experimental Safety Vehicles,* DOT, NHTSA.

Vasvada, A.N., Li, S. & Delp, S.L. (2001). Three-Dimensional isometric strength of neck muscles in humans. *Spine, 26(17),* 1904-1909.

Viano, D.C., Pellman, E.J., Withnall, C., Shewchenko, N., Bir, C.A., & Halstead, P.D. (2005). Concussion in professional football: Helmet testing to assess impact performance – Part 11. *Neurosurgery, 58,* 78-96.

Willinger, R., Baumgartner, D., Chinn, B., & Schuller, E. (2000). New dummy prototype: development, validation and injury criteria. *International Journal of Crashworthiness, 6(3),* 281-294

Yoganandan, N., Pintar, F.A., Sances, A., Walsh, P.R., Ewing, C.L., Thomas, D.J. et al. (1995). Biomechanics of skull fracture. *Journal of Neurotrauma, 12*(4), 659-668.

Zhang, L., Yang, K.H., & King, A.I. (2004). A proposed injury threshold for mild traumatic brain injury. *Journal of Biomechanical Engineering, 126,* 226-236.

Zhang, L., Yang, K.H., & King, A.I. (2001). Comparison of brain responses between frontal and lateral impacts by finite element modeling. *Journal of Neurotrauma, 18(1),* 21-30.

APPENDIX A

Hybrid III 50th percentile Headform Validation
For Front Location

Serial # AA0668-1

Product Validation Report

First Technology
Innovative Solutions

FTSS - Plymouth
ATD Certification Lab
47460 Galleon Drive
Plymouth, MI 48170

Cert ID:	0
Test ID:	197460
Test Date:	05/12/2009
Test Time:	03:37 PM

Test: Hybrid III 50th, Head, Front

Customer: Inventory
Serial Number: AA0668-1 Head B
Part Condition: New Spare
Corridor Type: NHTSA
Work Instruction: TLWI-1100

Test Result Details

Parameter Description	Test Point	Unit	Low	Result	High	Unit	Result
Resultant Acceleration	0.00		225	238.75	275	g	Pass
Lateral Acceleration	0.00		-15	13.70	15	g	Pass
Unimodal Oscillation	0.00		0	3.68	10	%	Pass
Temperature	0.00		18.9	21.5	25.6	degC	Pass
Humidity	0.00		10	25.0	70	%	Pass

Test Setup Details

Channel	Channel Name	Sensor SN	Axis	Cal Due Date	Gain	Filter	Class
1	Trigger	100000	None	03/30/10	1.0099	3000	None
2	X-Axis	J37684	None	09/05/09	50.7437	3000	1000
3	Y-Axis	P49430	None	09/05/09	200.847	3000	1000
4	Z-Axis	J36875	None	09/05/09	50.8374	3000	1000

Test Uncertainty Ratio (TUR) is greater than 4:1 with a 95% confidence level.

Comments:

Certified by: John Rdzanek **Signature:**

TESTING CERT
#1650.02

First Technology Safety Systems 47460 Galleon Dr. Plymouth, MI 48170 Phone: 1-451-9549

NOTICE
This certificate may not be reproduced, except in full, without written approval from the test lab
The test results on this page relate only to the serial number listed above

Printed on 5/12/2009

Cert ID	Test ID	Part Serial #	ATD Serial #	ATD Type	Test Date	Test Time
0	197460		AA0668-1	Hybrid III 50th	05/12/2009	03 37 PM

Filtered Data - Hybrid III 50th Head Front

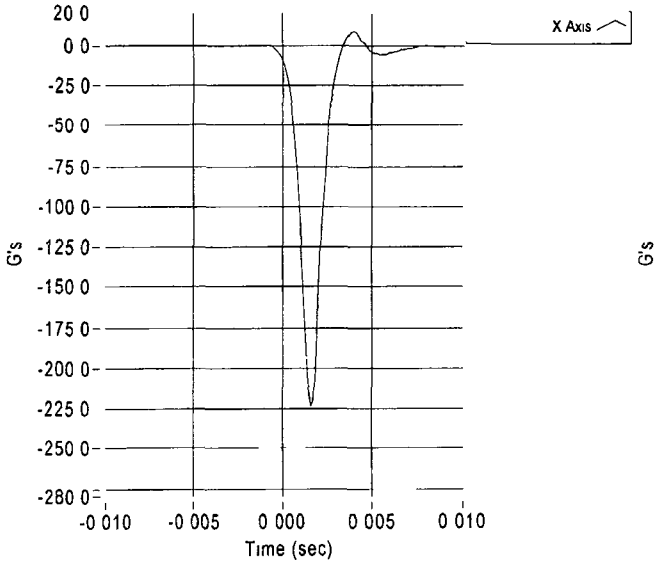

Filtered Data - Hybrid III 50th Head Front

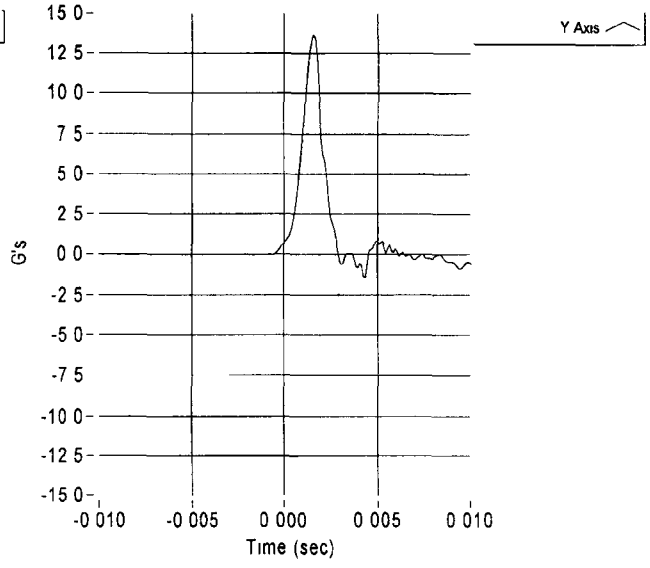

Filtered Data - Hybrid III 50th Head Front

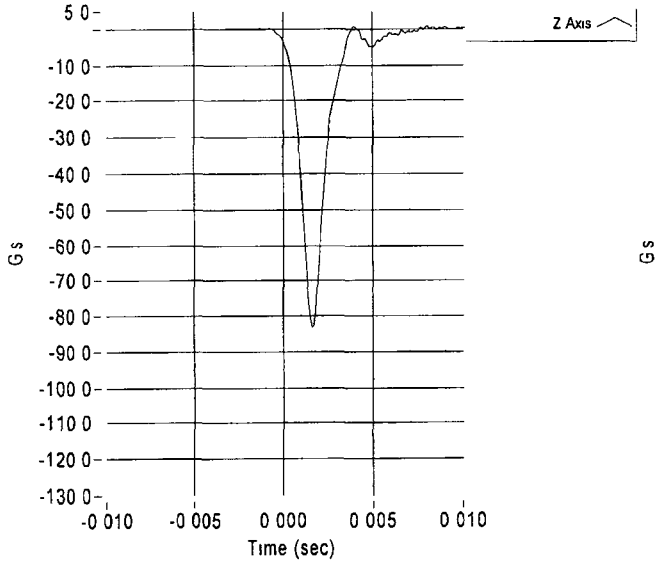

Resultant Data - Hybrid III 50th Head Front

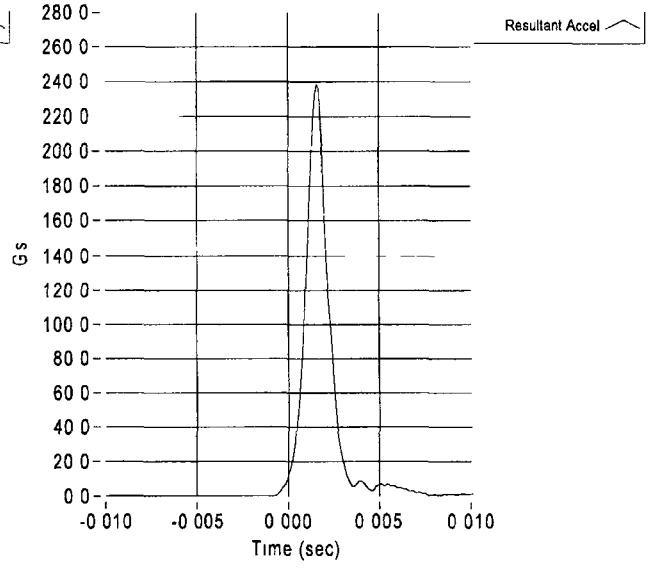

APPENDIX B

Hybrid III 50th percentile Neck Validation
For Flexion & Extension

Serial # 4859

Neck Pendulum Test Stand

Model Number: TF-200-0000

DENTON

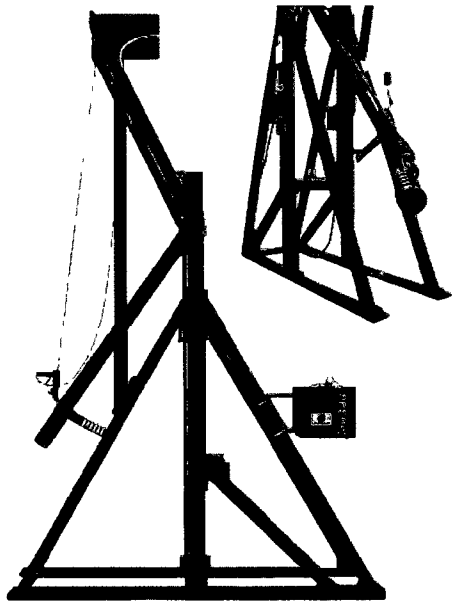

DESCRIPTION

The neck pendulum test is accomplished by releasing the pendulum and allowing it to fall freely to achieve a given impact velocity. The aluminum honeycomb stops the pendulum with a specified acceleration versus time pulse.

Velocity measurements are made by means of an infrared velocity measurement system. This system is made up of an infrared emitter, detector, and a precision slotted vane. The slotted vane is attached to the pendulum, and when dropped, the vane passes between the infrared emitter and detector generating a series of on/off pulses that can be converted into velocity by the data acquisition system.

Honeycomb material is positioned on four (4) aluminum dowel pins mounted on the face of the back stop which locates this material in the proper position between the pendulum striker plate and the back stop.

An upper neck load cell and one uniaxial accelerometer required for the test are not included.

Dimensions	Fixture	Work Area
Length	11.0 ft	13.0 ft
Width	2.5 ft	5.0 ft
Height	12.9 ft	—

INTRODUCTION

The TF-200 Neck Pendulum Test Stand is a complete system used for the calibration and testing of the neck component for the Hybrid III family, Hybrid II 50th, SA-106C, SA-103C, BioSID, EuroSID-1, ES-2, SID-HIII and SID-IIs. The neck can be tested in both the flexion and extension modes. The neck performance specifications for these tests are velocity at impact, pendulum acceleration, total rotation of the head/neck system, moment about the occipital condyle, and force.

The neck pendulum is in compliance with the specifications as written in the United States Code of Federal Regulation, Title 49, Part 572 relating to weight, center-of-gravity, moment of inertia, and mounting location of the pendulum accelerometer.

Standard Equipment

- 'A' frame welded steel structure
- Pendulum assembly; Part 572 compliant
- Structural back stop
- Infrared velocity measurement system
- Mechanical Angle Indicator
- Torque wrench 0 - 30 in-lb.
- Calibration unit for potentiometers
- Condyle Pin Removal Fixture
- Scissors

Optional Equipment

- Neck Mounting Adaptation packages are available for the following dummies:
  - * Hybrid III 50th/Hybrid III 95th
  - * Hybrid III 5th
  - * Hybrid III 10 Y.O.
  - * Hybrid III 6 Y.O.
  - * Hybrid III 3 Y.O.
  - * CRABI 12-Month-Old
  - * Hybrid II 50th
  - * SA-106C
  - * SA-103C
  - * SID-HIII
  - * SID-IIs
  - * EuroSID-1
  - * ES-2
- Hybrid III 5th/Hybrid III 6 Y.O. Adapter Plate for condyle pin removal fixture
- Aluminum honeycomb 4 ft x 8 ft x 6 inches
- Aluminum honeycomb 4 ft x 8 ft x 3 inches
- Electric hoist
- Electro-mechanical quick release
- Electronic inclinometer with display
- Pendulum rope hoist with snap release mechanism

Denton ATD, Inc. 10317 U.S. Highway 250 North, Milan, Ohio 44846-9570
Tel (419) 625-5200 * Fax (419) 625-5335 * email: info@dentonatd.com * www.dentonatd.com

Creating the New Standard in ATDs

Revision 06/19/06

Product Validation Report

First Technology
Innovative Solutions

FTSS - Plymouth
ATD Certification Lab
47460 Galleon Drive
Plymouth, MI 48170

Cert ID:	0
Test ID:	181523
Test Date:	08/30/2008
Test Time:	08:41 AM

Test: Hybrid III 50th, Neck, Neck Flexion

Customer: Inventory
Serial Number: 4859-1
Part Condition: New Spare
Corridor Type: NHTSA
Work Instruction: TLWI-1200

Test Result Details

Parameter Description	Test Point	Unit	Low	Result	High	Unit	Result
Velocity	0.00		6.89	6.97	7.13	m/sec	Pass
Pendulum Deceleration at	10.00	mSec	22.5	26.48	27.5	g	Pass
Pendulum Deceleration at	20.00	mSec	17.6	19.98	22.6	g	Pass
Pendulum Deceleration at	30.00	mSec	12.5	12.99	18.5	g	Pass
Max Pendulum Decel After	30.00	mSec	0	12.87	29	g	Pass
Decel Curve Decay Time to	5.00	g	34	37.60	42	mSec	Pass
Max D-Plane Rotation	0.00		64	74.90	78	degree	Pass
Time at Peak Rotation	0.00		57	60.30	64	mSec	Pass
D-Plane Rotation Crossing	0.00	degre	113	119.00	128	mSec	Pass
Max Occipital Moment	0.00		88.1	94.07	108.4	N-m	Pass
Time at Max Moment	0.00		47	49.00	58	mSec	Pass
Occipital Moment Crossing	0.00	mSec	97	100.30	107	mSec	Pass
Temperature	0.00		20.6	21.2	22.2	degC	Pass
Humidity	0.00		10	40.0	70	%	Pass

Test Setup Details

Channel	Channel Name	Sensor SN	Axis	Cal Due Date	Gain	Filter	Class
9	Velocity	NeckVel2	None	06/13/09	1	3000	None
10	Moment, My	226	My	11/26/08	500	3000	600
11	Force, Fx	226	Fx	11/26/08	500	3000	1000
14	Pendulum Pot	3PP2	None	10/04/08	2	3000	60
15	Head Pot	3HP2	None	10/04/08	2	3000	60
13	Pendulum Accel	C14920	None	12/12/08	100	3000	60

Test Uncertainty Ratio (TUR) is greater than 4:1 with a 95% confidence level.

Comments:

Certified by: John Ruzanek **Signature:**

TESTING CERT
#1850.02

NOTICE
This certificate may not be reproduced, except in full, without written approval from the test lab
The test results on this page relate only to the serial number listed above

Cert ID	Test ID	Part Serial #	ATD Serial #	ATD Type	Test Date	Test Time
0	181523		4859-1	Hybrid III 50th	08/30/2008	08:41 AM

Filtered Data - Hybrid III 50th Neck Neck Flexion

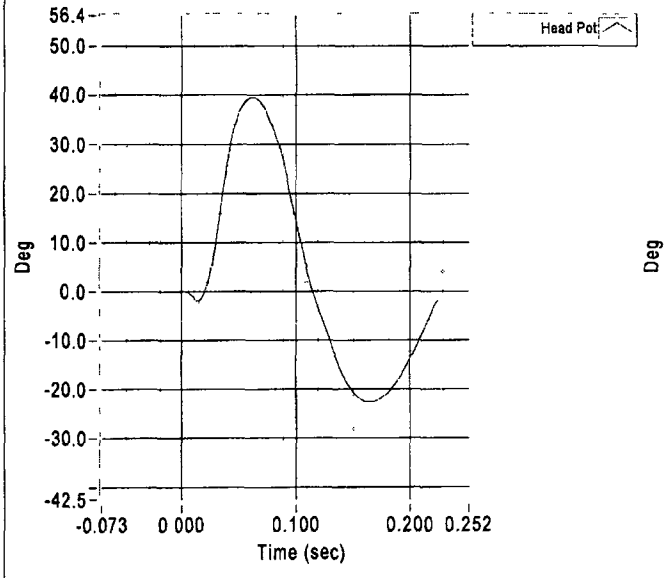

Filtered Data - Hybrid III 50th Neck Neck Flexion

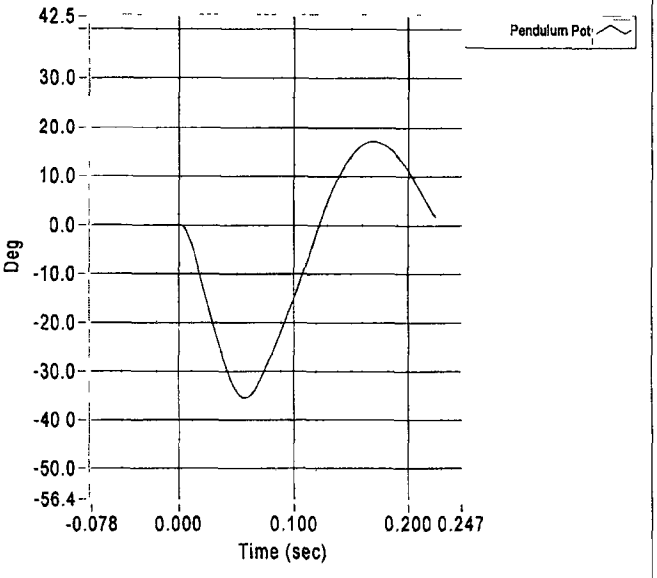

Resultant Data - Hybrid III 50th Neck Neck Flexion

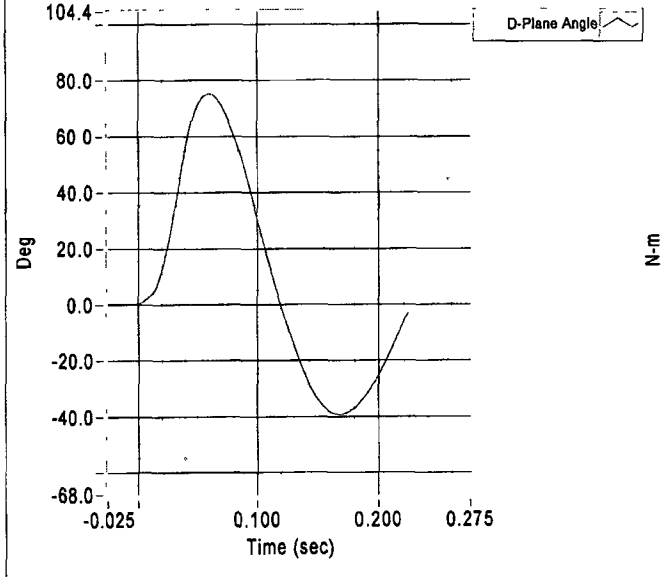

Filtered Data - Hybrid III 50th Neck Neck Flexion

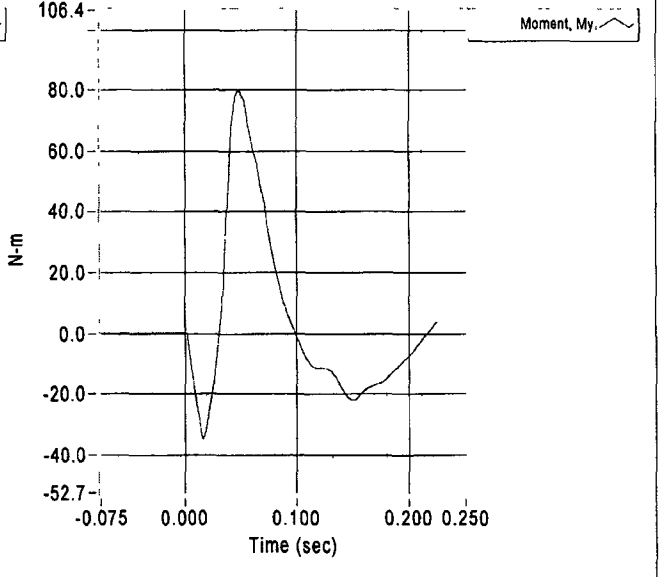

Cert ID	Test ID	Part Serial #	ATD Serial #	ATD Type	Test Date	Test Time
0	181523		4859-1	Hybrid III 50th	08/30/2008	08:41 AM

Filtered Data - Hybrid III 50th Neck Neck Flexion

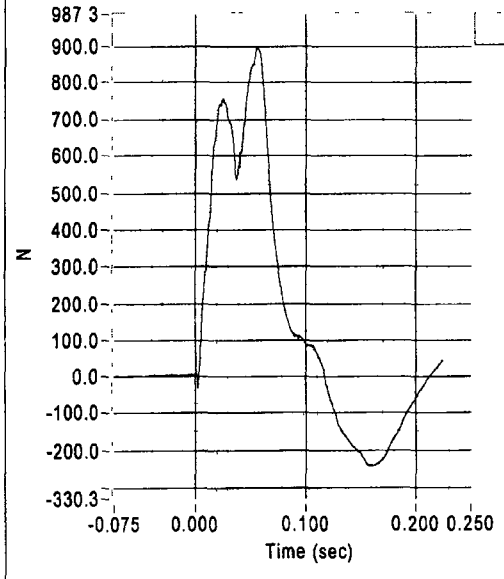

Resultant Data - Hybrid III 50th Neck Neck Flexion

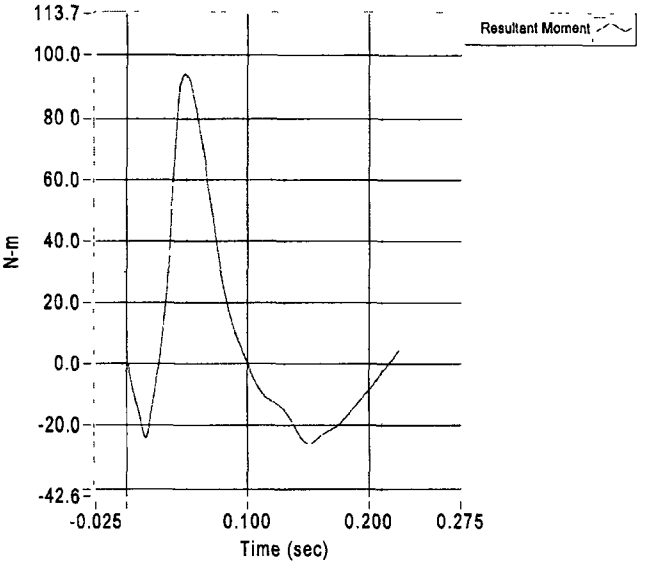

Filtered Data - Hybrid III 50th Neck Neck Flexion

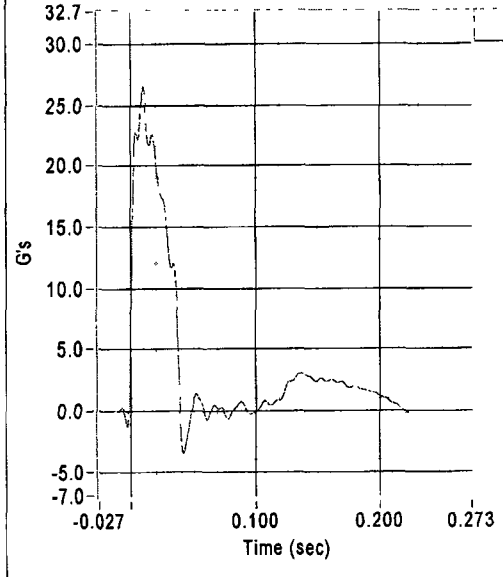

Resultant Data - Hybrid III 50th Neck Neck Flexion

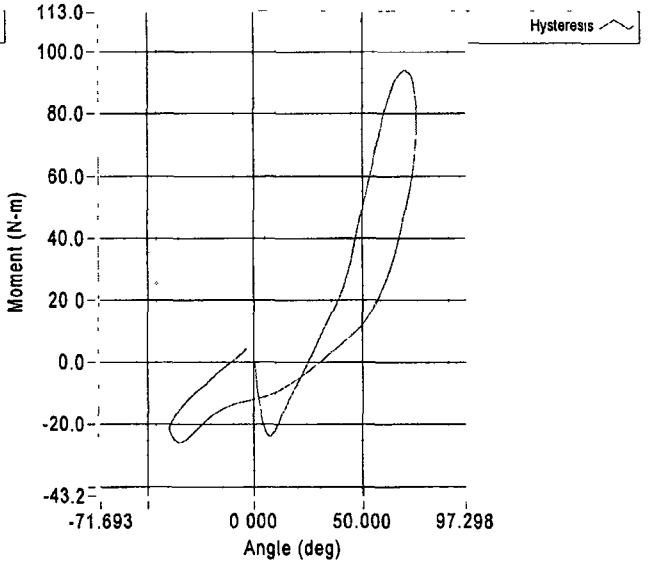

Product Validation Report

First Technology
Innovative Solutions

FTSS - Plymouth
ATD Certification Lab
47460 Galleon Drive
Plymouth, MI 48170

Cert ID:	0
Test ID:	181532
Test Date:	08/30/2008
Test Time:	11:35 AM

Test: Hybrid III 50th, Neck, Neck Extension

Customer: Inventory
Serial Number: 4859-2
Part Condition: New Spare
Corridor Type: NHTSA
Work Instruction: TLWI-1200

Test Result Details

Parameter Description	Test Point	Unit	Low	Result	High	Unit	Result
Velocity	0.00		5.95	6.09	6.19	m/sec	Pass
Pendulum Deceleration at	10.00	mSec	17.2	19.73	21.2	g	Pass
Pendulum Deceleration at	20.00	mSec	14	16.55	19	g	Pass
Pendulum Deceleration at	30.00	mSec	11	12.22	16	g	Pass
Max Pendulum Decel After	30.00	mSec	0	12.78	22	g	Pass
Decel Curve Decay Time to	5.00	g	38	41.00	46	mSec	Pass
Max D-Plane Rotation	0.00		81	93.13	106	degree	Pass
Time at Peak Rotation	0.00		72	76.30	82	mSec	Pass
D-Plane Rotation Crossing	0.00	degre	147	159.80	174	mSec	Pass
Max Occipital Moment	0.00		-80	-72.05	-53	N-m	Pass
Time at Max Moment	0.00		65	72.50	79	mSec	Pass
Occipital Moment Crossing	0.00	mSec	120	145.70	148	mSec	Pass
Temperature	0.00		20.6	21.2	22.2	degC	Pass
Humidity	0.00		10	40.0	70	%	Pass

Test Setup Details

Channel	Channel Name	Sensor SN	Axis	Cal Due Date	Gain	Filter	Class
9	Velocity	NeckVel2	None	06/13/09	1	3000	None
10	Moment, My	226	My	11/26/08	500	3000	600
11	Force, Fx	226	Fx	11/26/08	500	3000	1000
14	Pendulum Pot	3PP2	None	10/04/08	2	3000	60
15	Head Pot	3HP2	None	10/04/08	2	3000	60
13	Pendulum Accel	C14920	None	12/12/08	100	3000	60

Test Uncertainty Ratio (TUR) is greater than 4:1 with a 95% confidence level.

Comments:

Certified by: John Rdzanek **Signature:**

TESTING CERT
#1050.02

First Technology Safety Systems 47460 Galleon Dr. Plymouth, MI 48170 Phone: +1 51-9549

NOTICE
This certificate may not be reproduced, except in full, without written approval from the test lab
The test results on this page relate only to the serial number listed above

Cert ID	Test ID	Part Serial #	ATD Serial #	ATD Type	Test Date	Test Time
0	181532		4859-2	Hybrid III 50th	08/30/2008	11:35 AM

Filtered Data - Hybrid III 50th Neck Neck Extension

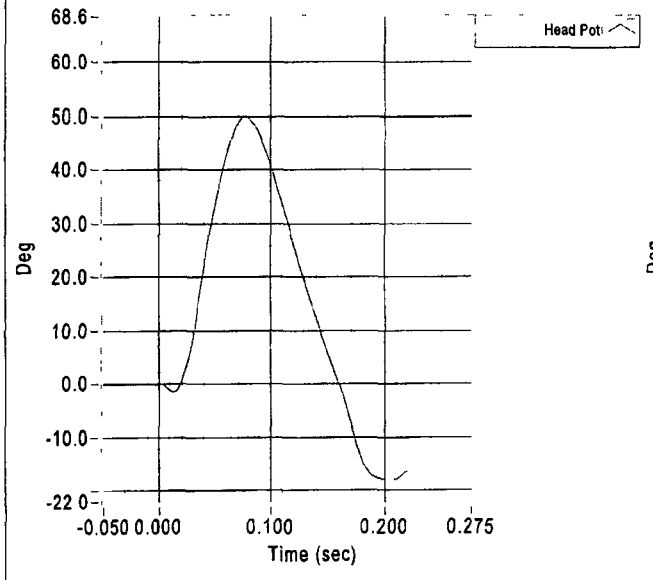

Filtered Data - Hybrid III 50th Neck Neck Extension

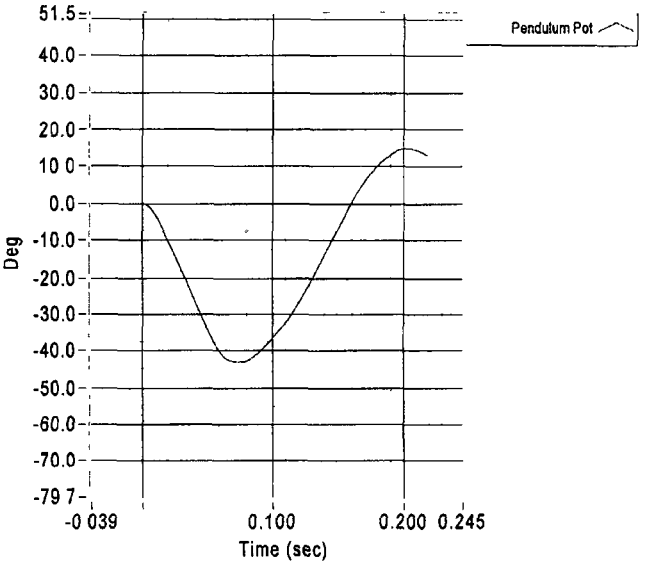

Resultant Data - Hybrid III 50th Neck Neck Extension

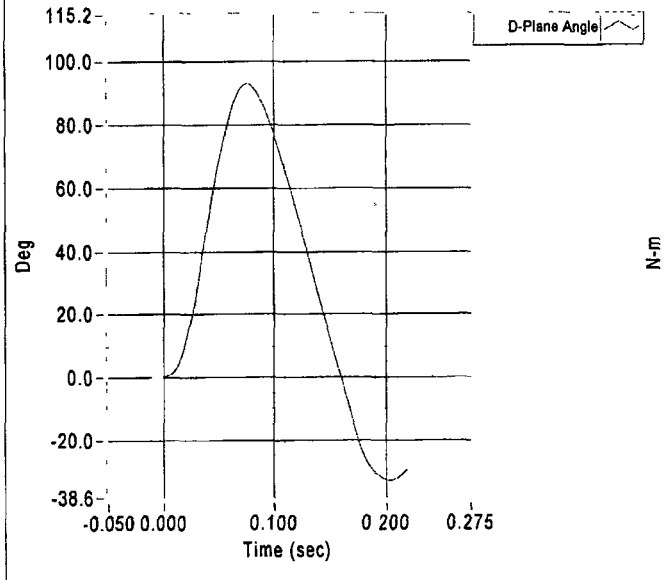

Filtered Data - Hybrid III 50th Neck Neck Extension

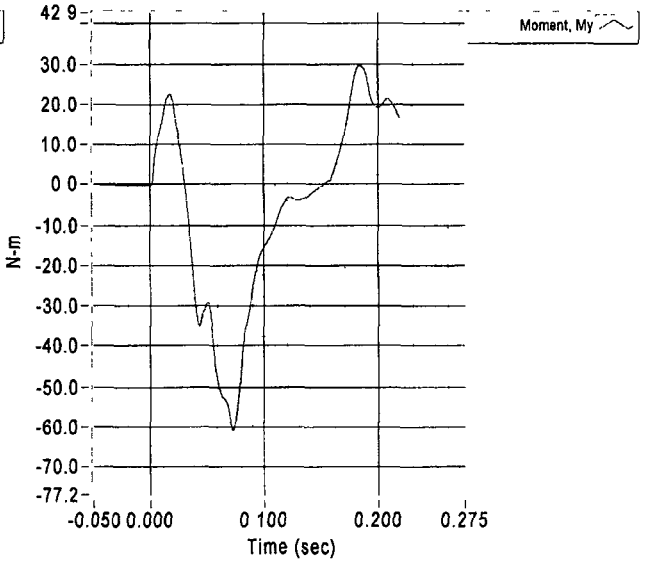

Cert ID	Test ID	Part Serial #	ATD Serial #	ATD Type	Test Date	Test Time
0	181532		4859-2	Hybrid III 50th	08/30/2008	11:35 AM

Filtered Data - Hybrid III 50th Neck Neck Extension

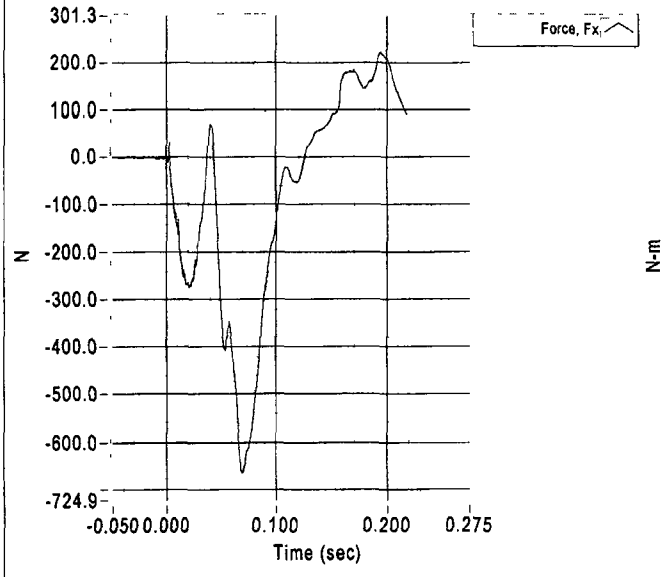

Resultant Data - Hybrid III 50th Neck Neck Extension

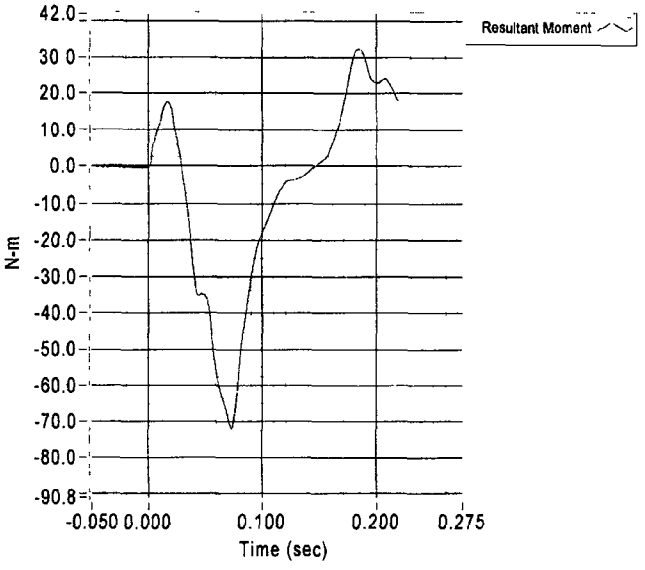

Filtered Data - Hybrid III 50th Neck Neck Extension

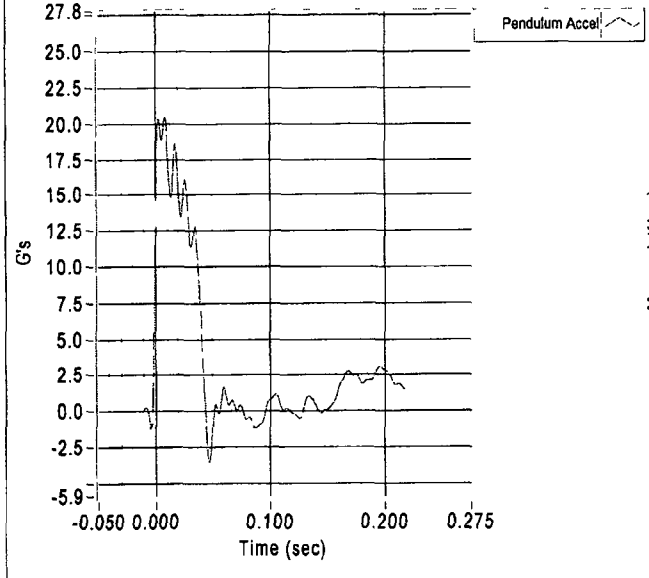

Resultant Data - Hybrid III 50th Neck Neck Extension

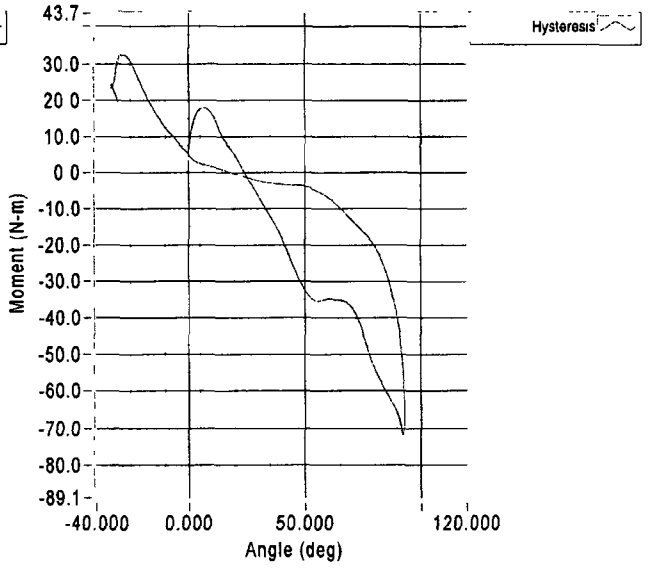

APPENDIX C

Hybrid III 50th percentile Neck Validation
For Flexion, Extension and Lateral Bending using Instron

Serial # 4859

Hybrid III Neckform #4859 Quasi-static Validation using Instron

Quasi-static validation of the Hybrid III neckform was performed using an Instron material tester. The Hybrid III was placed in a jig (Figure 1) perpendicular to the line of draw. A cable was attached to the neck and was deflected at a rate of 100mm/min displacing 40mm. A load deflection curve was produced to demonstrate the varying compliances of the different neck orientations. The rearward neck orientation was found to be most stiff, where the forward neck orientation was the softest, relatively (Figure 2).

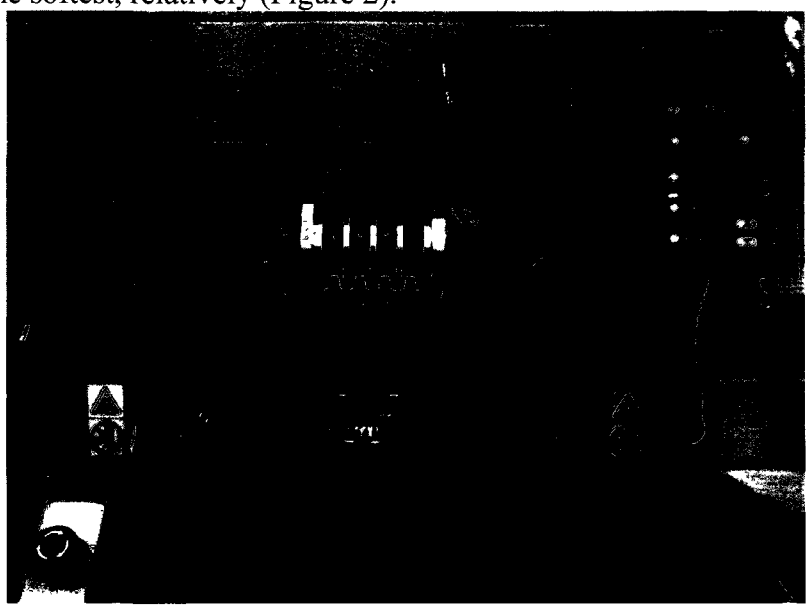

Figure 1: Instron machine with Hybrid III neckform in jig ready for load deflection testing.

Test Information	
Hybrid III Neckform Serial #:	4859
Rate (mm/min):	100
Displacement (mm):	40
Maximum Load (N):	300N

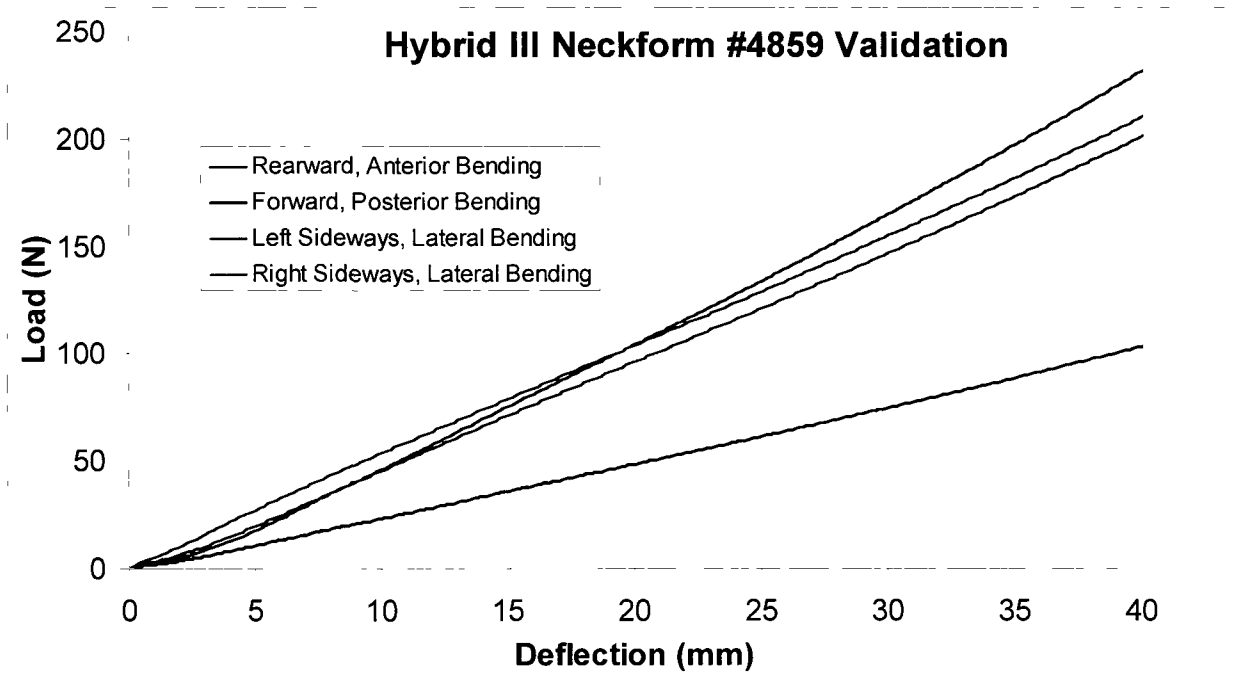

Figure 2. Each line represents the load/deflection curve of each Hybrid III neckform orientation.